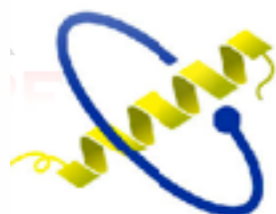


Membrane protein megahertz crystallography at the European XFEL

Nadia Zatsepin

La Trobe University

EuXFEL Users' Meeting 2020



CENTRE FOR ADVANCED
MOLECULAR IMAGING
AN ARC CENTRE OF EXCELLENCE

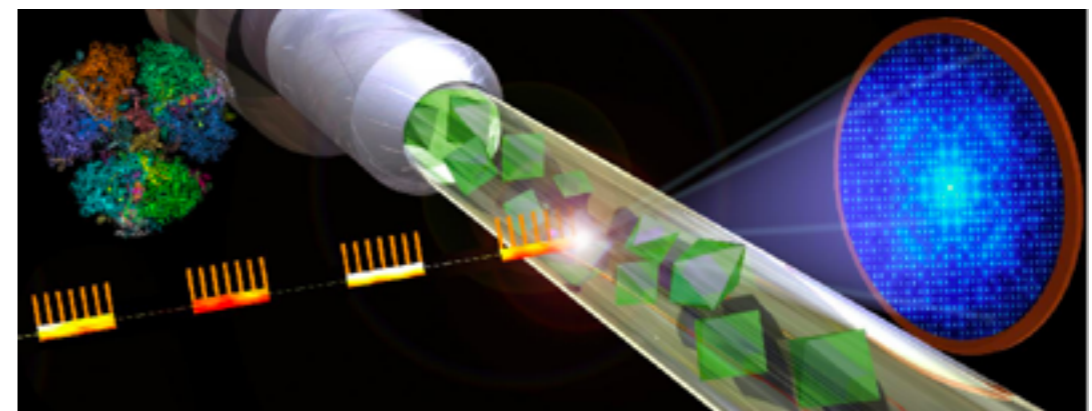


This work is the culmination of almost a decade of XFEL crystallography development



Gisriel et al. Nat Comm. 10, 5021 (2019).

Chris Gisriel, Jesse Coe, Romain Letrun, Oleksandr M. Yefanov, Cesar Luna-Chavez, Natasha E. Stander, Stella Lisova, Valerio Mariani, Manuela Kuhn, Steve Aplin, Thomas D. Grant, Katerina Dörner, Tokushi Sato, Austin Echelmeier, Jorvani Cruz Villarreal, Mark S. Hunter, Max O. Wiedorn, Juraj Knoska, Victoria Mazalova, Shatabdi Roy-Chowdhury, Jay-How Yang, Alex Jones, Richard Bean, Johan Bielecki, Yoonhee Kim, Grant Mills, Britta Weinhausen, Jose D. Meza, Nasser Al-Qudami, Saša Bajt, Gerrit Brehm, Sabine Botha, Djelloul Boukhelef, Sandor Brockhauser, Barry D. Bruce, Matthew A. Coleman, Cyril Danilevski, Erin Discianno, Zachary Dobson, Hans Fangohr, Jose M. Martin-Garcia, Yaroslav Gevorkov, Steffen Hauf, Ahmad Hosseinizadeh, Friederike Januschek, Gihan K. Ketawala, Christopher Kupitz, Luis Maia, Maurizio Manetti, Marc Messerschmidt, Thomas Michelat, Jyotirmoy Mondal, Abbas Ourmazd, Gianpietro Previtali, Iosifina Sarrou, Silvan Schön, Peter Schwander, Megan L. Shelby, Alessandro Silenzi, Jolanta Sztuk-Dambietz, Janusz Szuba, Monica Turcato, Thomas A. White, Krzysztof Wrona, Chen Xu, Mohamed H. Abdellatif, James D. Zook, John C. H. Spence, Henry N. Chapman, Anton Barty, Richard A. Kirian, Matthias Frank, Alexandra Ros, Marius Schmidt, Raimund Fromme, Adrian P. Mancuso, **Petra Fromme** & Nadia A. Zatsepin



Acknowledgements

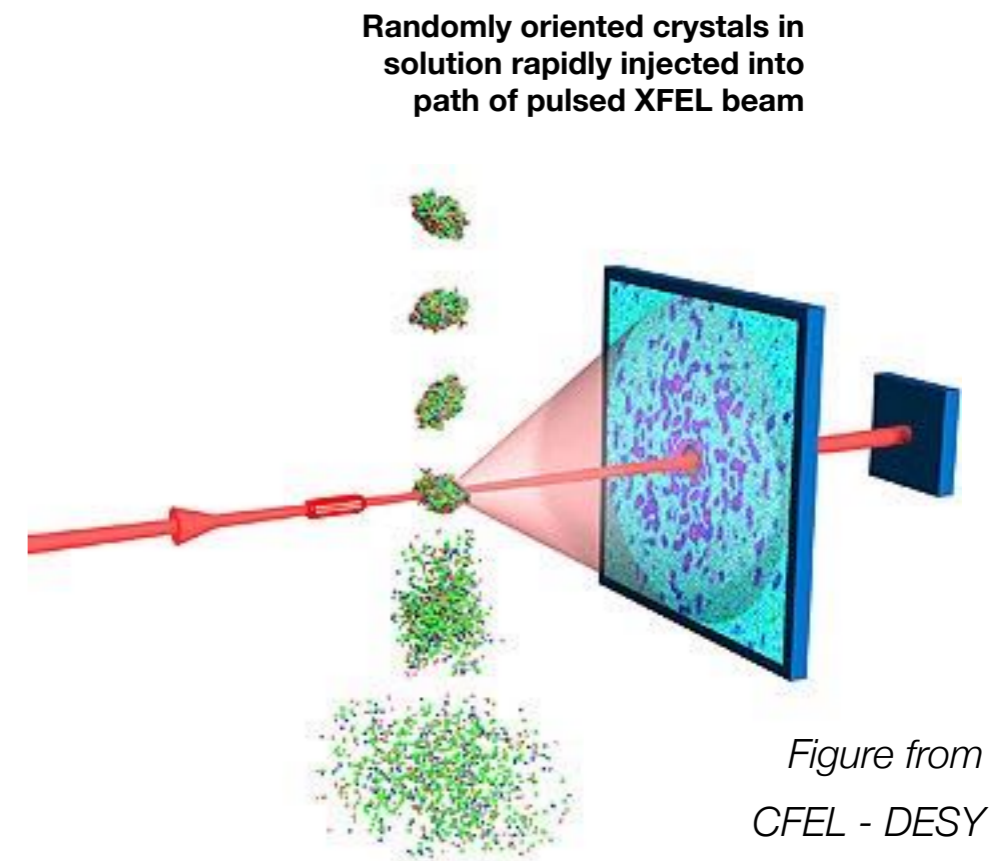
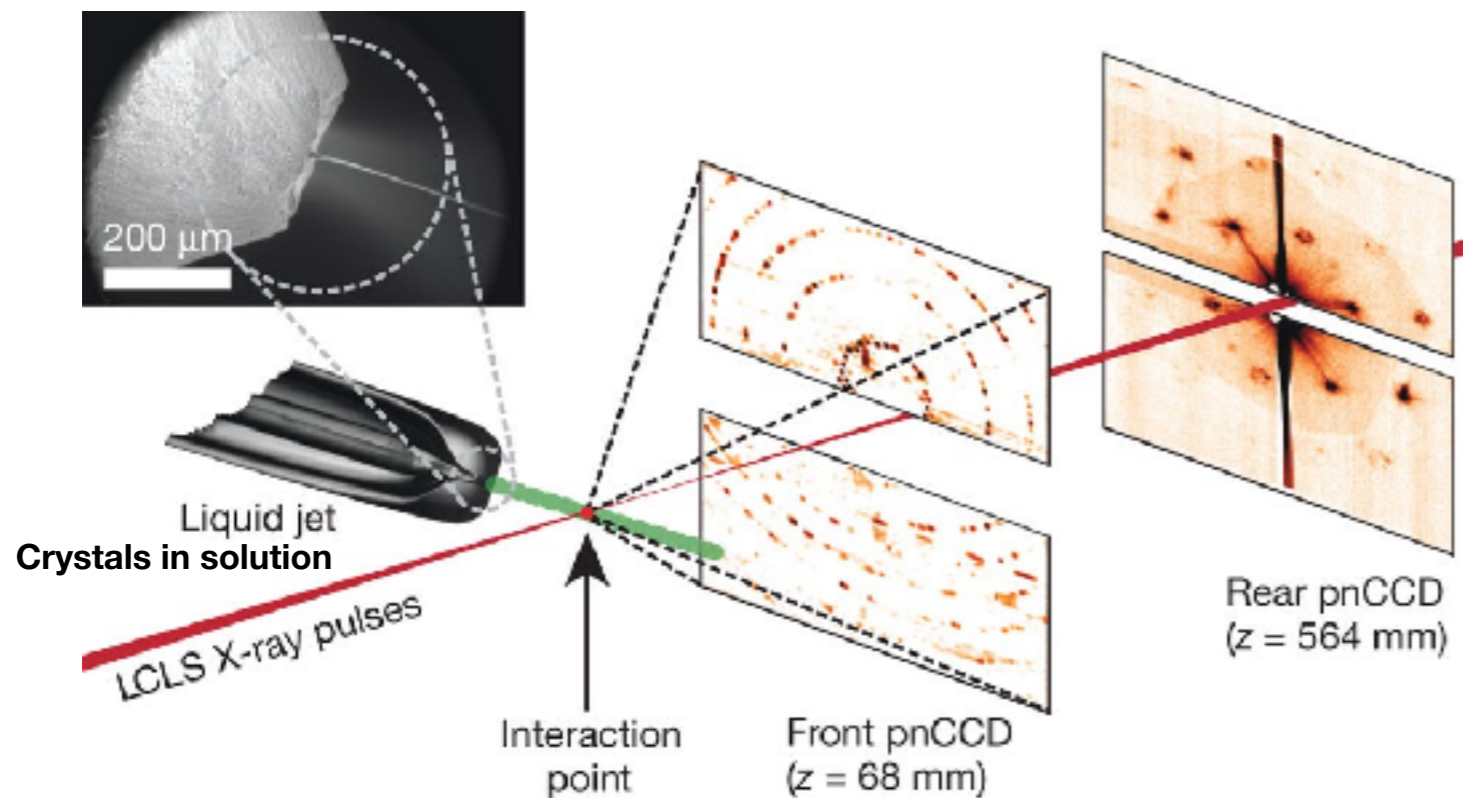
Chris Gisriel^{1,2,23,26}, Jesse Coe^{1,2,26}, Romain Letrun³, Oleksandr M. Yefanov⁴, Cesar Lunda-Chavez^{1,2}, Natasha E. Stander^{1,2}, Stella Lisova^{1,5}, Valerio Mariani⁴, Manuela Kuhn⁴, Steve Aplin⁴, Thomas D. Grant^{6,7}, Katerina Dörner³, Tokushi Sato^{3,4}, Austin Echelmeier^{1,2}, Jorvani Cruz Villarreal^{1,2}, Mark S. Hunter⁸, Max O. Wiedorn^{4,9,10}, Juraj Knoska⁴, Victoria Mazalova⁴, Shatabdi Roy-Chowdhury^{1,2}, Jay-How Yang^{1,2}, Alex Jones^{1,2}, Richard Bean³, Johan Bielecki³, Yoonhee Kim³, Grant Mills³, Britta Weinhausen³, Jose D. Meza³, Nasser Al-Qudami³, Saša Bajt¹¹, Gerrit Brehm^{1,2,12,13}, Sabine Botha⁵, Djelloul Boukhelef³, Sandor Brockhauser^{3,14}, Barry D. Bruce^{15,16,17}, Matthew A. Coleman¹⁸, Cyril Danilevski³, Erin Discianno¹, Zachary Dobson^{1,2}, Hans Fangohr^{3,19}, Jose M. Martin-Garcia¹, Yaroslav Gevorkov^{4,20}, Steffen Hauf³, Ahmad Hosseinizadeh²¹, Friederike Januschek^{3,24}, Gihan K. Ketawala^{1,2}, Christopher Kupitz^{8,21}, Luis Maia³, Maurizio Manetti³, Marc Messerschmidt^{1,2,3}, Thomas Michelat³, Jyotirmoy Mondal¹⁵, Abbas Ourmazd²¹, Gianpietro Previtali³, Iosifina Sarrou⁴, Silvan Schön⁴, Peter Schwander²¹, Megan L. Shelby¹⁸, Alessandro Silenzi³, Jolanta Sztuk-Dambietz³, Janusz Szuba³, Monica Turcato³, Thomas A. White⁴, Krzysztof Wrona³, Chen Xu³, Mohamed H. Abdellatif⁴, James D. Zook^{1,2}, John C.H. Spence^{1,5}, Henry N. Chapman^{4,9,10}, Anton Barty⁴, Richard A. Kirian^{1,5}, Matthias Frank¹⁸, Alexandra Ros^{1,2}, Marius Schmidt²¹, Raimund Fromme^{1,2}, Adrian P. Mancuso^{3,22}, Petra Fromme^{1,2*} & Nadia A. Zatsepin^{1,5,25*}

¹Biodesign Center for Applied Structural Discovery, Arizona State University, Tempe, AZ 85287-5001, USA. ²School of Molecular Sciences, Arizona State University, Tempe, AZ 85287-1604, USA. ³European XFEL GmbH, Holzkoppel 4, 22869 Schenefeld, Germany. ⁴Center for Free-Electron Laser Science, Deutsches Elektronen-Synchrotron, Notkestrasse 85, 22607 Hamburg, Germany. ⁵Department of Physics, Arizona State University, Tempe, AZ 85287-1504, USA. ⁶Hauptman-Woodward Institute, 700 Ellicott St, Buffalo, NY 14203-1102, USA. ⁷Department of Structural Biology, Jacobs School of Medicine and Biomedical Sciences, SUNY University at Buffalo, 700 Ellicott St, Buffalo, NY 14203-1102, USA. ⁸Linac Coherent Light Source, SLAC National Accelerator Laboratory, Menlo Park 94025 CA, USA. ⁹Department of Physics, Universität Hamburg, Luruper Chaussee 149, 22761 Hamburg, Germany. ¹⁰The Hamburg Centre for Ultrafast Imaging, Universität Hamburg, Luruper Chaussee 149, 22761 Hamburg, Germany. ¹¹Deutsches Elektronen-Synchrotron, Notkestrasse 85, 22607 Hamburg, Germany. ¹²Institute for X-Ray Physics, University of Göttingen, 37077 Göttingen, Germany. ¹³Center Nanoscale Microscopy and Molecular Physiology of the Brain, Göttingen, Germany. ¹⁴Biological Research Centre, Hungarian Academy of Sciences, Temesvári krt. 62, Szeged 6726, Hungary. ¹⁵Department of Biochemistry & Cellular and Molecular Biology, University of Tennessee at Knoxville, Knoxville, TN, USA 37996. ¹⁶Program in Energy Science and Engineering, University of Tennessee at Knoxville, Knoxville, TN, USA 37996. ¹⁷Department of Microbiology, University of Tennessee at Knoxville, Knoxville, TN, USA 37996. ¹⁸Lawrence Livermore National Laboratory, 7000 East Avenue, Livermore, CA 94550, USA. ¹⁹University of Southampton, University Rd, Southampton SO17 1BJ, UK. ²⁰Hamburg University of Technology, Vision Systems E-2, Harburger Schloßstraße 20, 21079 Hamburg, Germany. ²¹Department of Physics, University of Wisconsin-Milwaukee, 3135 N. Maryland Ave, Milwaukee, WI 53211, USA. ²²Department of Chemistry and Physics, La Trobe Institute for Molecular Science, La Trobe University, Melbourne 3086 Victoria, Australia. ²³Present address: Department of Chemistry, Yale University, New Haven, CT 06520, USA. ²⁴Present address: Deutsches Elektronen-Synchrotron, Notkestrasse 85, 22607 Hamburg, Germany. ²⁵Present address: Department of Chemistry and Physics, La Trobe Institute for Molecular Science, La Trobe University, Melbourne 3086 Victoria, Australia. ²⁶These authors contributed equally: Chris Gisriel, Jesse Coe.



Serial femtosecond crystallography

- Determine structures from nano/micro crystals, at room temperature
- **serial** delivery of micro-**crystals** (~ one crystal per one X-ray pulse)
- ~ 10 - 50 **fs X-ray pulses**

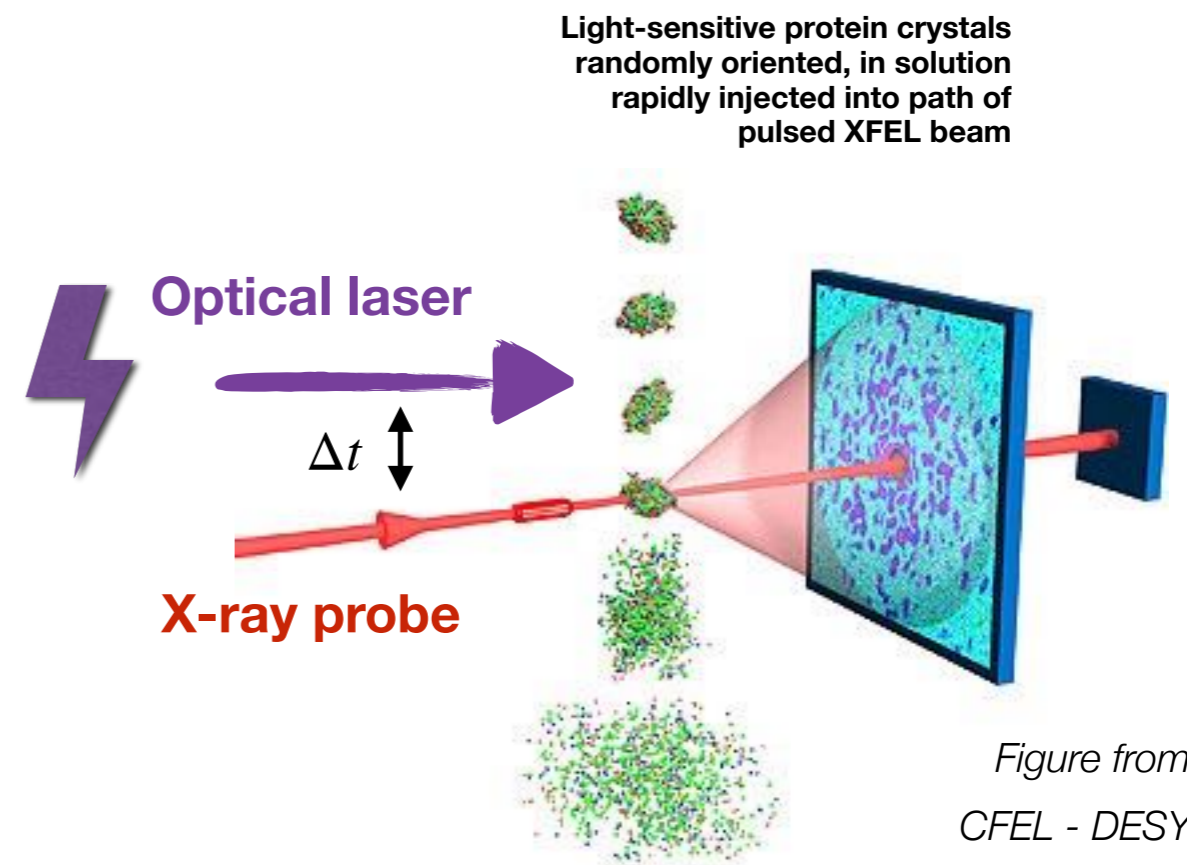


Chapman et al. Nature 470, 73 – 78 (2011).

Time-resolved Serial femtosecond crystallography

1. Initiate reaction by light, ligand mixing, temperature or pH jump
2. wait
3. collect diffraction snapshots of reaction intermediates
4. repeat for new time point

Pump-probe SFX :
light activated reactions



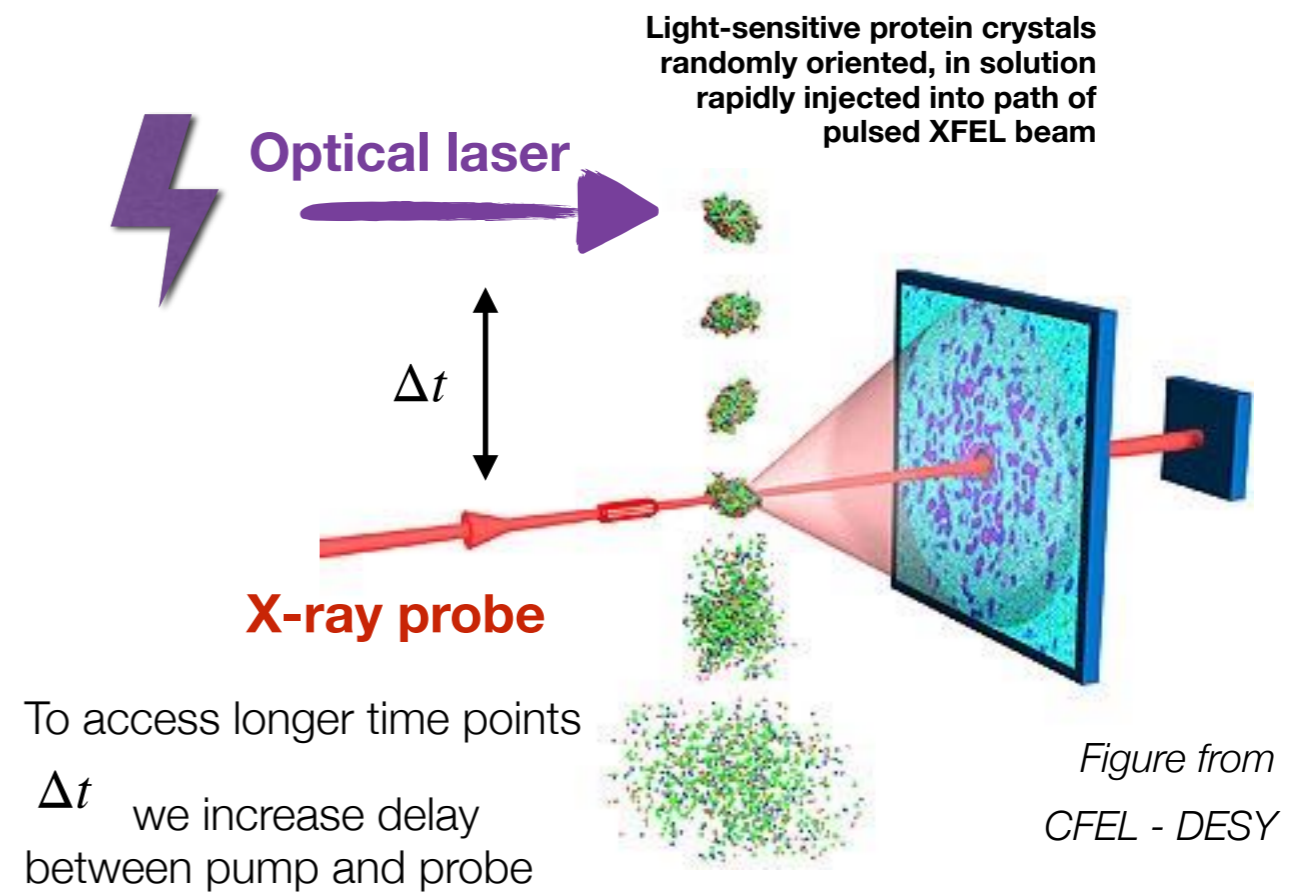
Pump-probe SFX:

See e.g. Tenboer et al. (2014) Science 346, 1242 and Pande et al. (2016) Science 352 (6268) and Pandey et al. (2020) TR-SFX from EuXFEL. Led by Marius Schmidt and the BioXFEL consortium.

Time-resolved Serial femtosecond crystallography

1. Initiate reaction by light, ligand mixing, temperature or pH jump
2. wait
3. collect diffraction snapshots of reaction intermediates
4. repeat for new time point

Pump-probe SFX :
light activated reactions

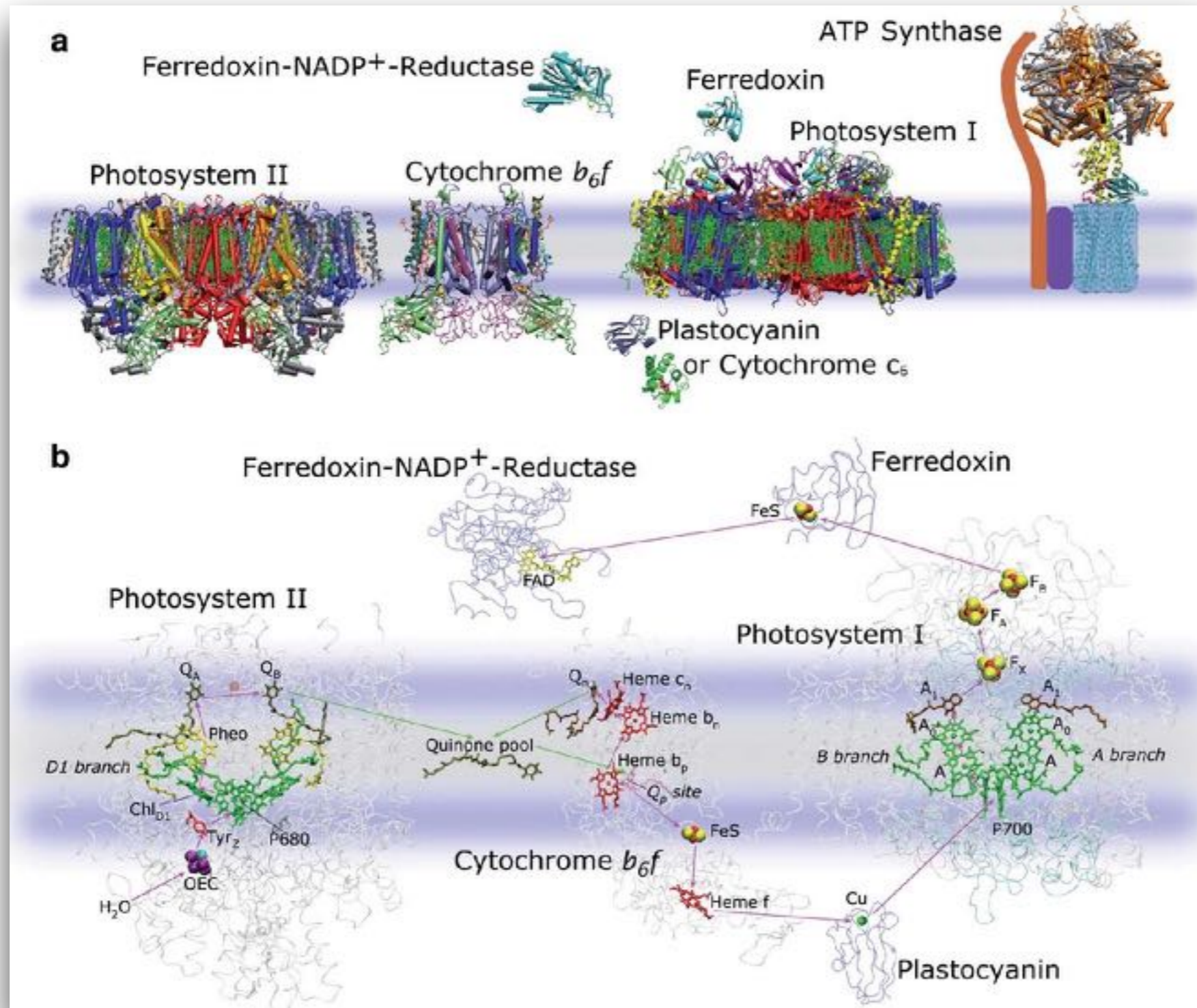


Pump-probe SFX:

See e.g. Tenboer et al. (2014) Science 346, 1242 and Pande et al. (2016) Science 352 (6268) and Pandey et al. (2020) TR-SFX from EuXFEL. Led by Marius Schmidt and the BioXFEL consortium.

Overview of oxygenic photosynthesis

Major components of the light reactions of cyanobacterial oxygenic photosynthesis



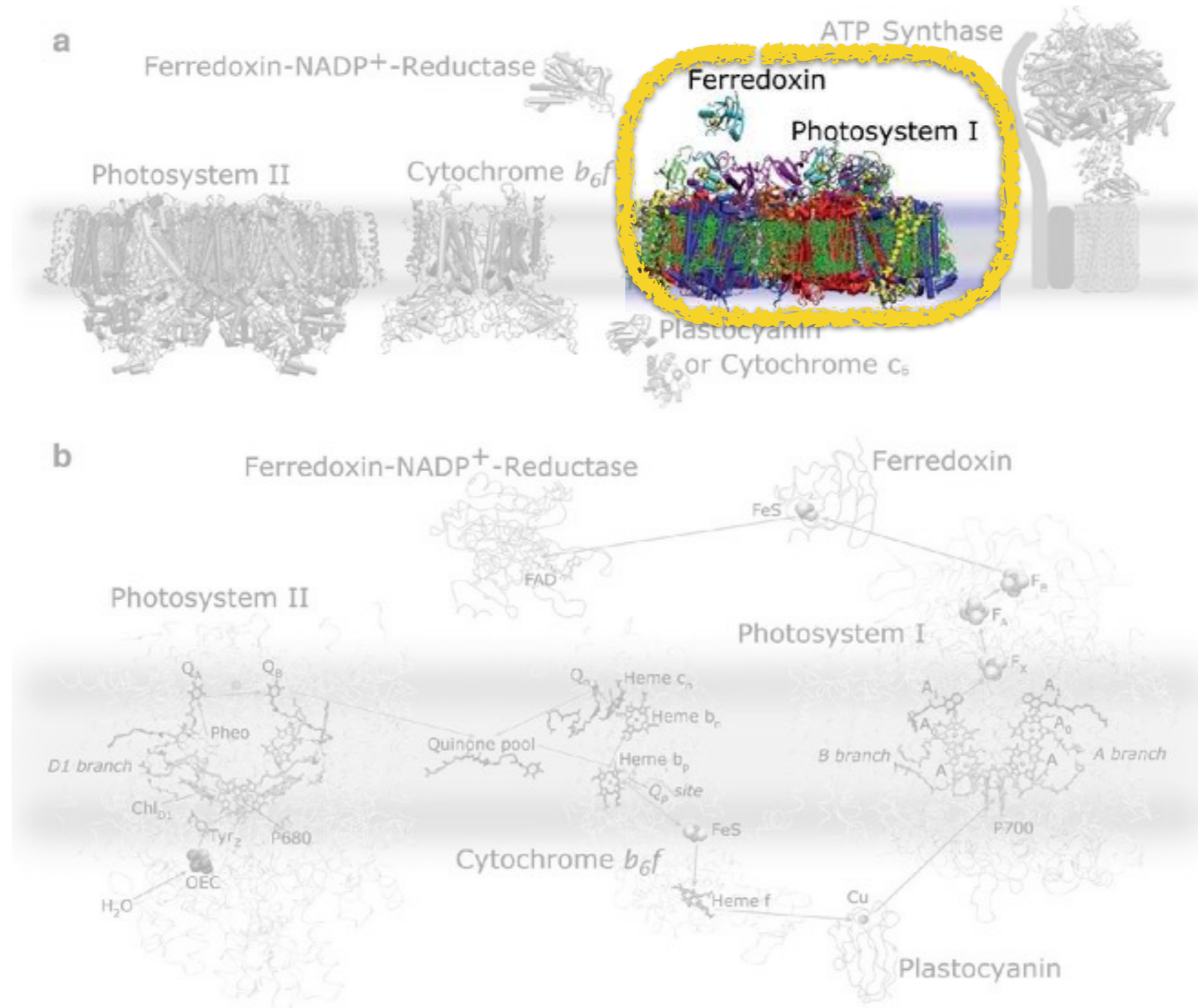
thylakoid membrane

Fromme lab

Figure from Ch. 1 Fromme & Grotjohann in Fromme P (ed.) *Photosynthetic Protein Complexes: A Structural Approach*. Wiley-Blackwell; 2008

Overview of oxygenic photosynthesis

Major components of the light reactions of cyanobacterial oxygenic photosynthesis

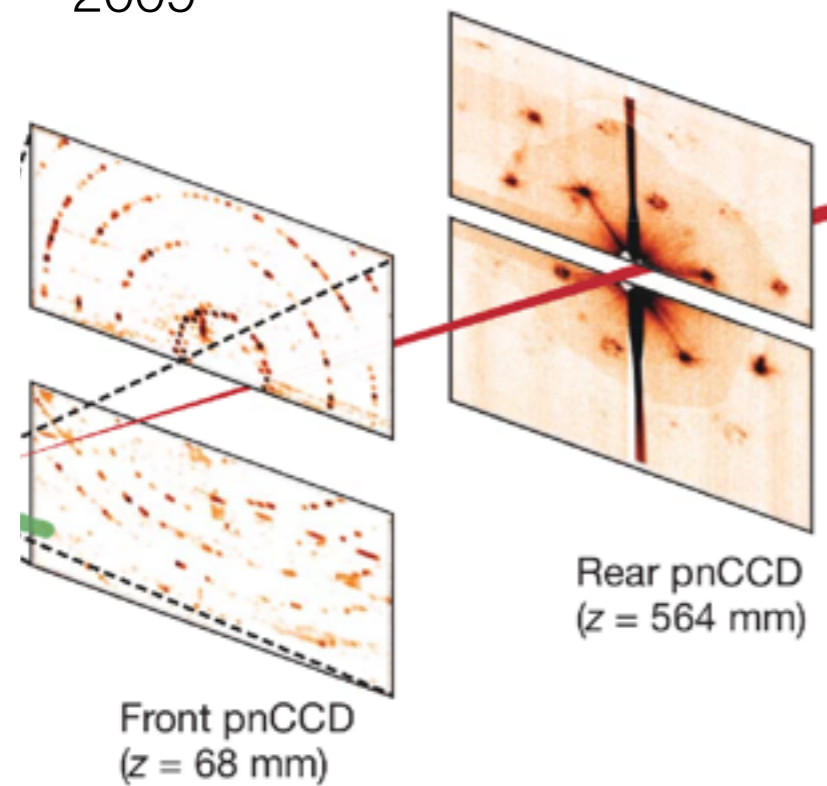


Fromme lab

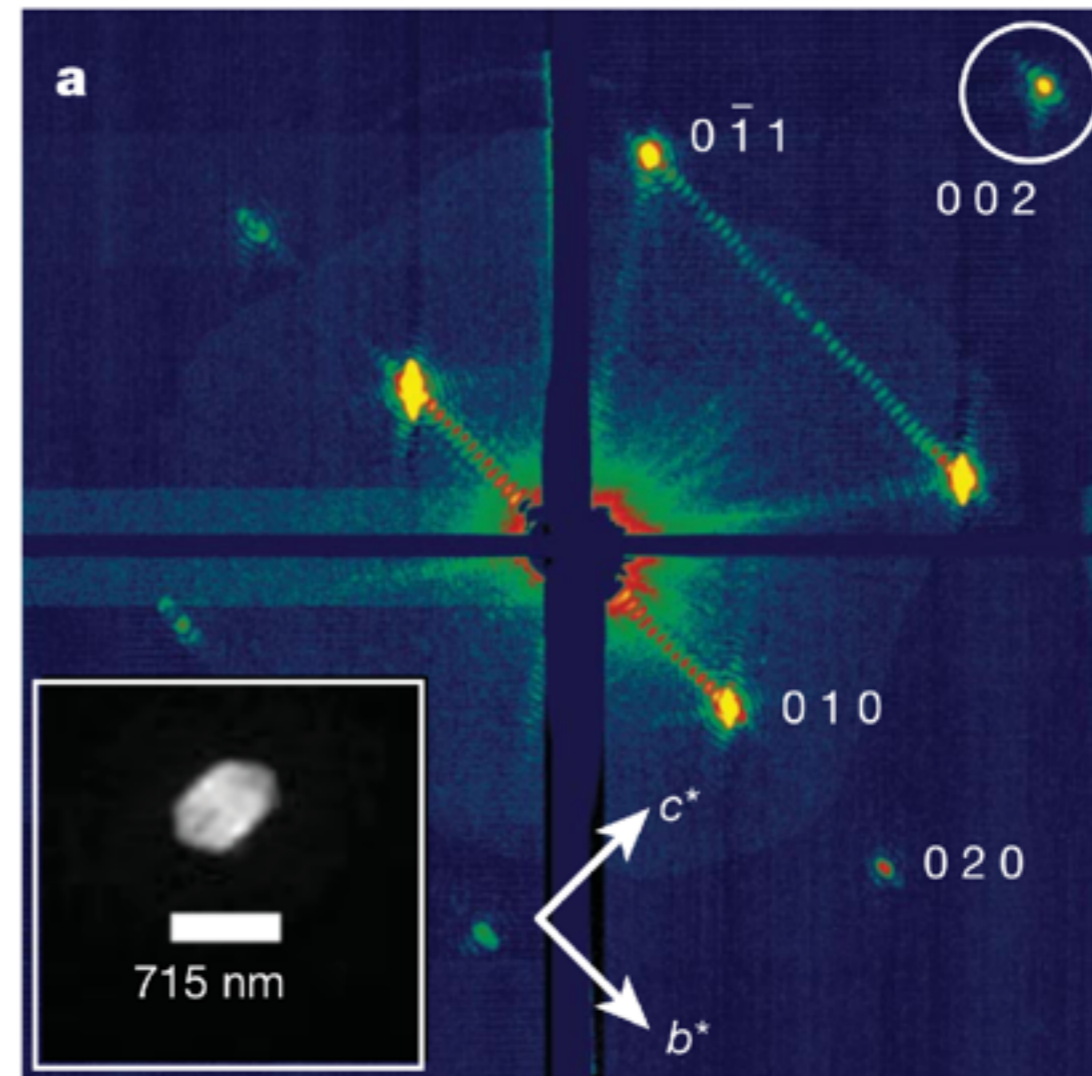
Figure from Ch. 1 Fromme & Grotjohann in Fromme P (ed.) *Photosynthetic Protein Complexes: A Structural Approach*. Wiley-Blackwell; 2008

SFX a decade ago

- Photosystem I nanocrystals were used for the very first SFX experiment:
 - 2 keV X-rays
 - AMO beam line at LCLS, in Dec 2009



- It became a high-precision detector geometry calibration tool...



But a high-resolution room temperature PSI structure was out of reach

Figures from Chapman et al. Nature 470, 73 – 78 (2011).

Photosystem I crystals

Photosystem I trimer
2.5 Å structure from crystals in space group P63
cyanobacteria *Thermosynechococcus elongatus*.
Jordan P. et.al, (2001) Nature 411, 909.

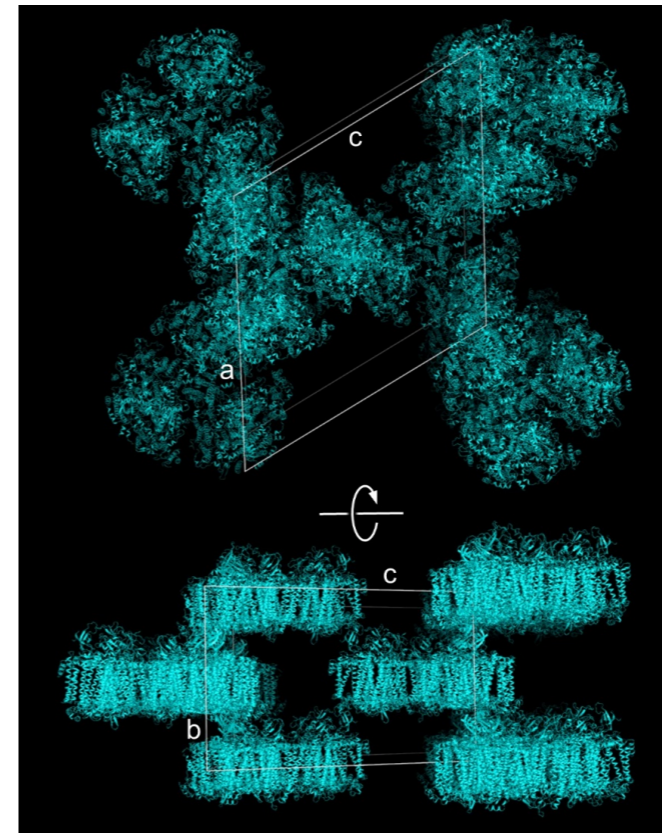
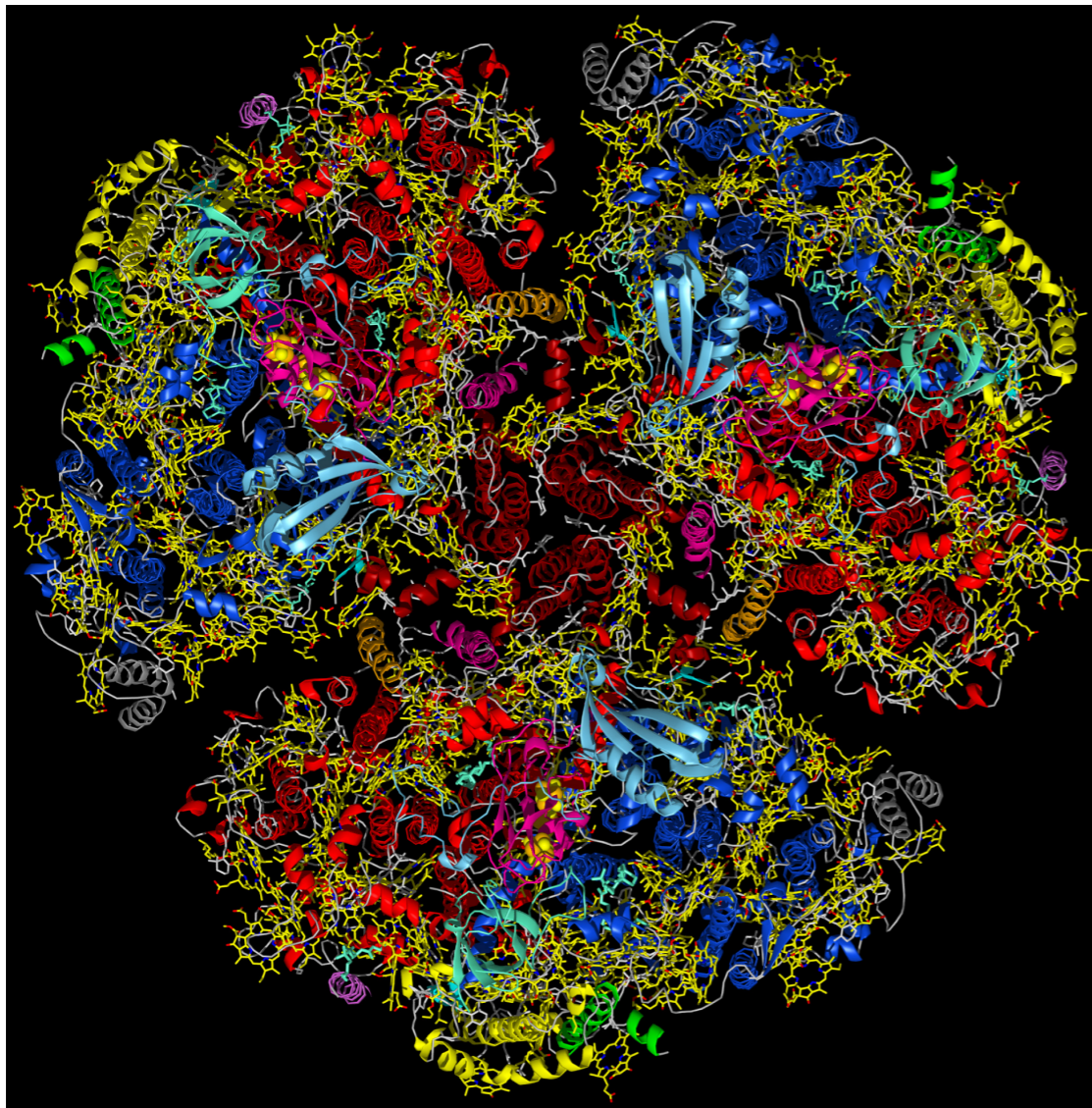


Figure from Gisriel et al. Nat Comm. 10, 5021 (2019).

PSI unit cell:

$$a = b = 281.0 \text{ \AA}$$

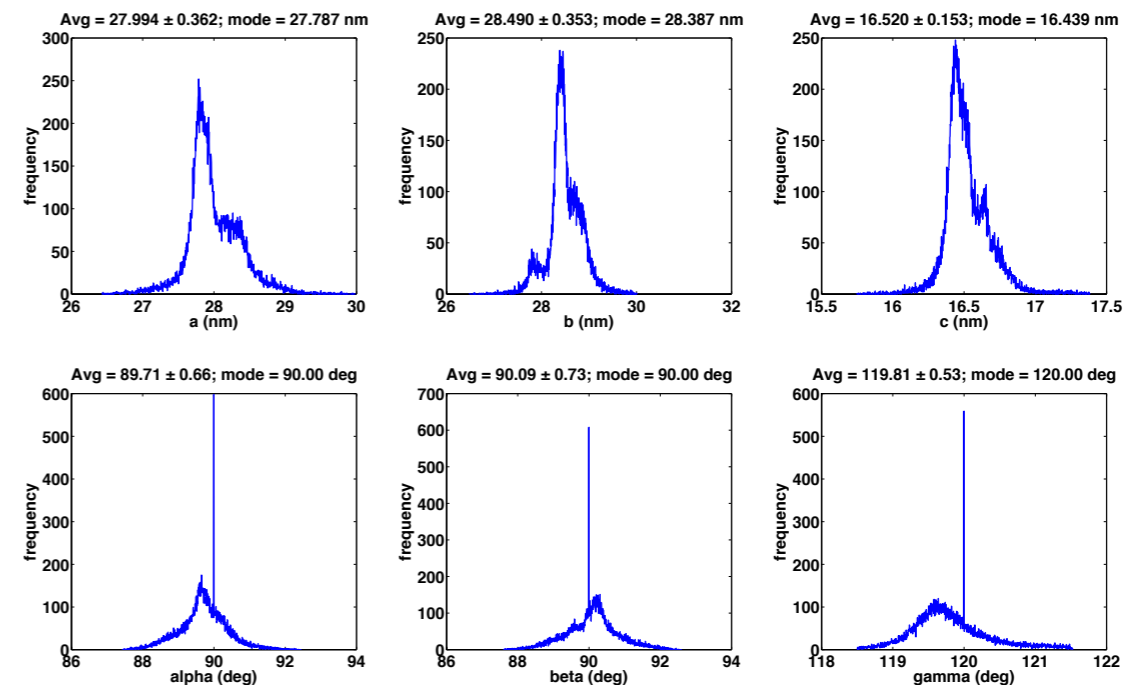
$$c = 165.2 \text{ \AA}$$

angles: 90, 90, 120.

- PSI trimer has > 72,500 atoms (excluding H).
- Molecular weight: 1.08 MDa.
- Very high solvent content: 78% --> flexible structure
- Very few crystal contacts (24)
- Large unit cell --> insufficient spot separation
- Often mosaic perpendicular to lipid membrane

Suspicious of pseudosymmetry

- **We saw hints of pseudo hexagonal PSI unit cell** since 2011 (at LCLS) but the SFX technique was very new and the **data were very noisy**.
- Since there was a 2.5 Å PSI P63 structure published, the conservative assumption was that it was **inaccurate detector geometry**, or **inaccurate SFX analysis** that created the appearance of loss of perfect hexagonal symmetry (i.e. that the PSI molecule is a slightly asymmetric trimer).
- It forced us to look very carefully at how we were (a) collecting the data (detector geometry), (b) indexing programs - some have preference for perfect symmetry; or we would impose it to guide the indexing, assuming P63 is right.
- In P63, the data would be "twinned by merohedry", i.e. appear to be in higher symmetry than real. We had no way of separating perfectly twinned snapshot (VERY noisy) SFX data. (We can solve this now using the CrystFEL program *ambigator*)



Unit cell distributions from PSI microcrystal SFX data in the early days (2012)

Trimeric PSI (pseudo-hexagonal P21) requires 3x more data

Major developments in SFX data analysis

- Detector geometry refined to sub-pixel accuracy
- Detector improvements
- Hit finding and detector calibration
 - Indexing algorithms: Xgandalf, MOSFLM updates
 - CrystFEL: detwinning (ambigator), diffraction geometry modeling, peak prediction accuracy, intensity scaling, B factor scaling,
 - DatView

Weierstall, U. *Liquid sample delivery techniques for serial femtosecond crystallography. Philos. Trans. R. Soc. B Biol. Sci.* 369, 20130337 (2014)

Yefanov, O. et al. *Accurate determination of segmented X-ray detector geometry. Opt. Express* 23, 28459–28470 (2015) --> **geoptimiser**

Mariani, V. et al. **OnDA**: online data analysis and feedback for serial X-ray imaging. *J. Appl. Cryst.* 49, 1073–1080 (2016)

Barty, A. et al. **Cheetah**: software for high-throughput reduction and analysis of serial femtosecond X-ray diffraction data. *J. Appl. Cryst.* 47, 1118–1131 (2014)

Gevorkov, Y. et al. **XGANDALF**—extended gradient descent algorithm for lattice finding. *Acta Crystallogr. Sect. A* 75, 694–704 (2019)

White, T. A. et al. Recent developments in **CrystFEL**. *J. Appl. Crystallogr.* 49, 680–689 (2016)

Stander, N. **DatView**: a graphical user interface for visualizing and querying large data sets in serial femtosecond crystallography. *J. Appl. Crystallogr.* 52, 1440–1448 (2019).

Major developments in XFELs

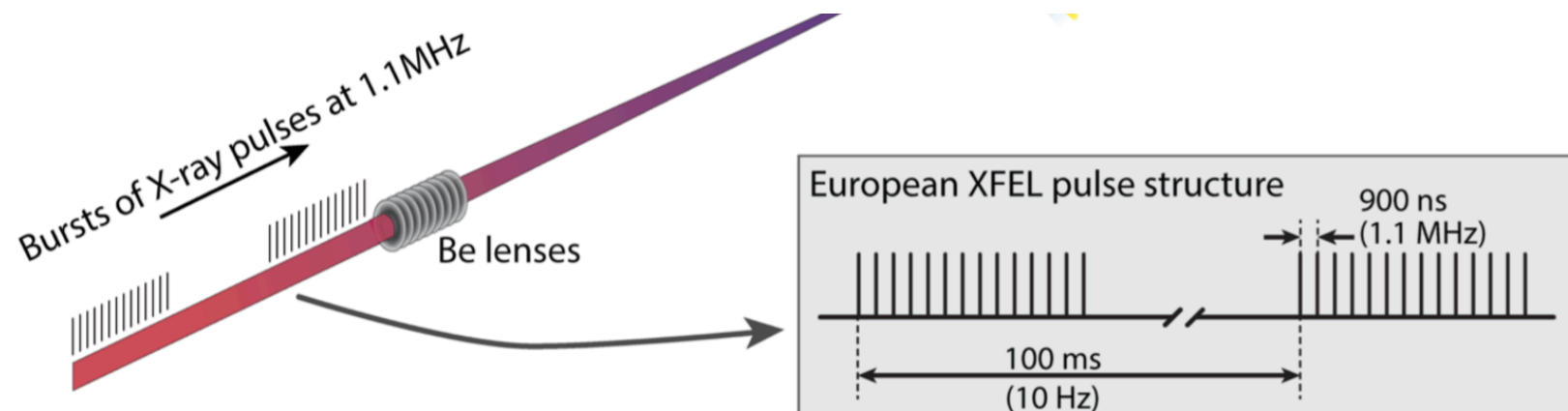
	Start of user operation	Pulse delivery	Maximum pulses per second	Minimum time between pulses (ms)
LCLS ^{1#}	2009	constant frequency	120	8.33
SACLA ^{2#}	2011	constant frequency	60	16.67
PAL-XFEL ^{3#}	2016	constant frequency	30	16.67
EuXFEL ^{4#*}	2017	pulse trains at 10 Hz	2,500 [#]	0.000886 [#]
			27,000 [*]	0.000222 [*]
SwissFEL ^{5#}	2018	constant frequency	100	10
LCLS-II ^{6*}	2021 [*]	constant frequency	1000000 [*]	0.001



Optimal sample delivery would lead to 1 crystal per shot, but the crystal size, sample delivery buffer and required **jet velocities of > 50 m/s** limit the achievable hit rate.

At EuXFEL sample must be replenished about 9000 faster than at LCLS. Large volumes of sample are wasted between pulse trains

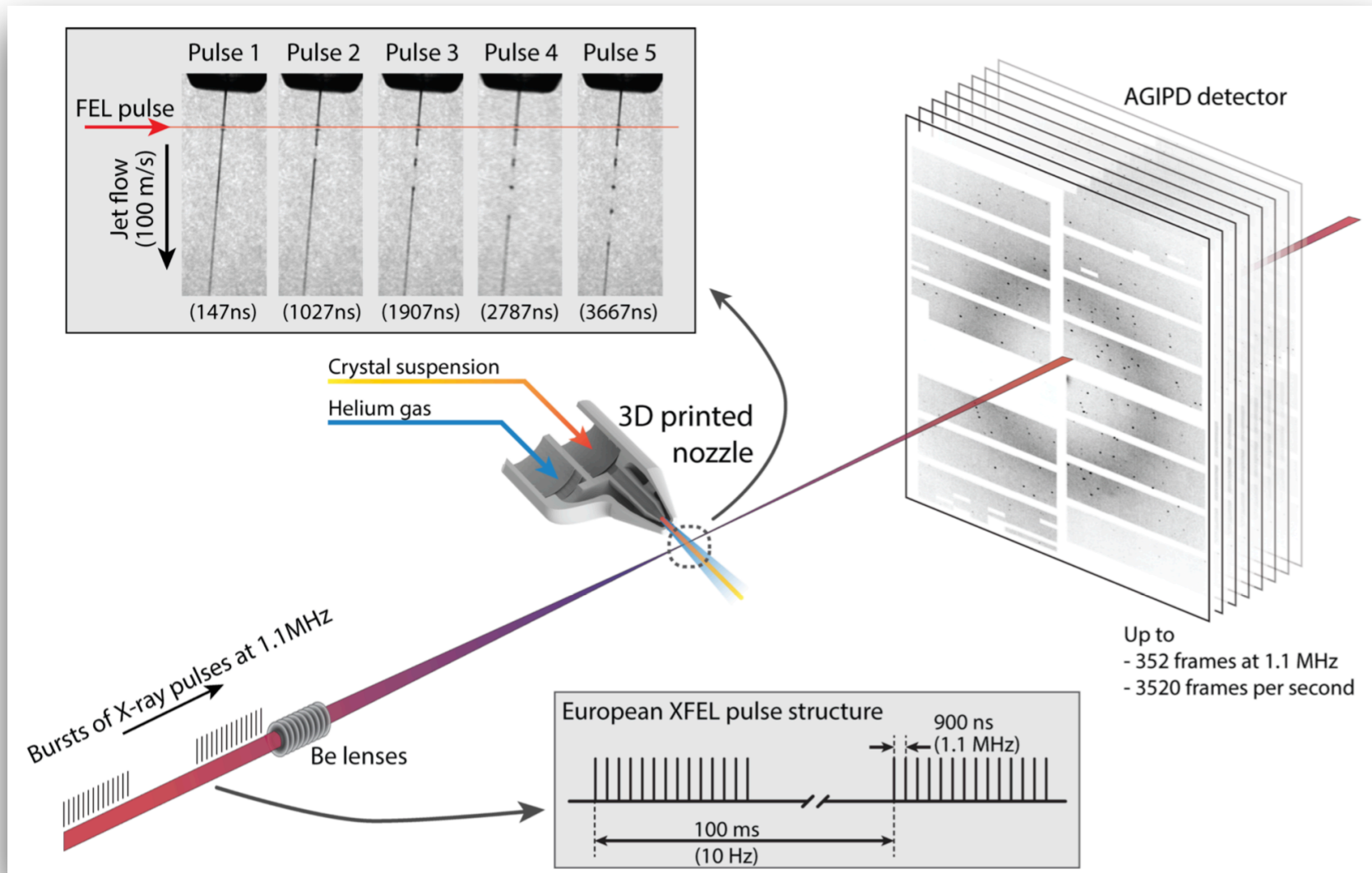
Alexandra Ros' lab (ASU) has developed & demonstrated a droplet injector interspersing sample-containing aqueous buffer droplets with oil: Sample is delivery at 10 Hz --> much less waste



Up to
 - 352 frames at 1.1 MHz
 - 3520 frames per second

Figure from Wiedorn, M. O. et al. Megahertz serial crystallography. Nat. Commun. 9, 4025 (2018)

High frequency XFEL pulses require high sample injection flow rates



Fast flow rates
require much more
sample

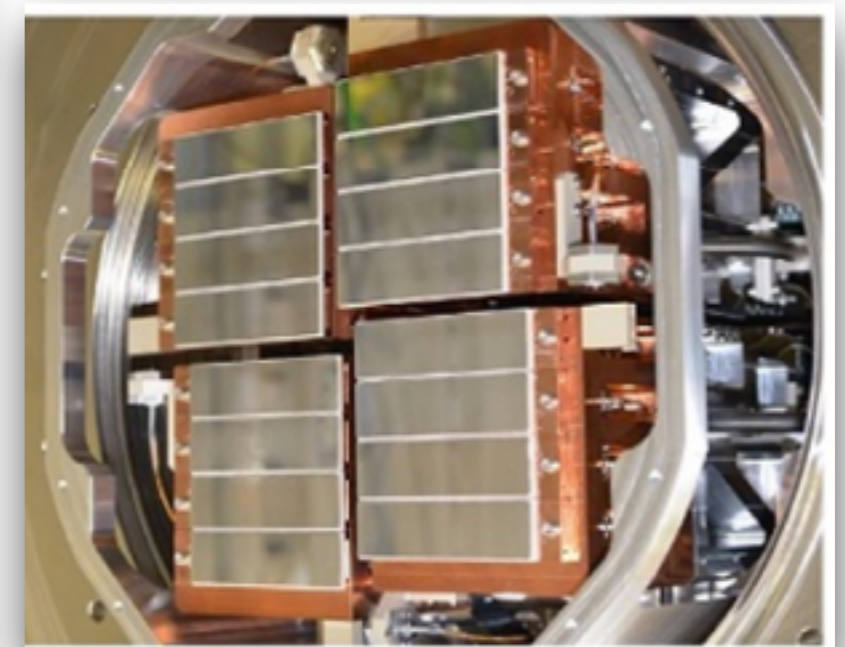


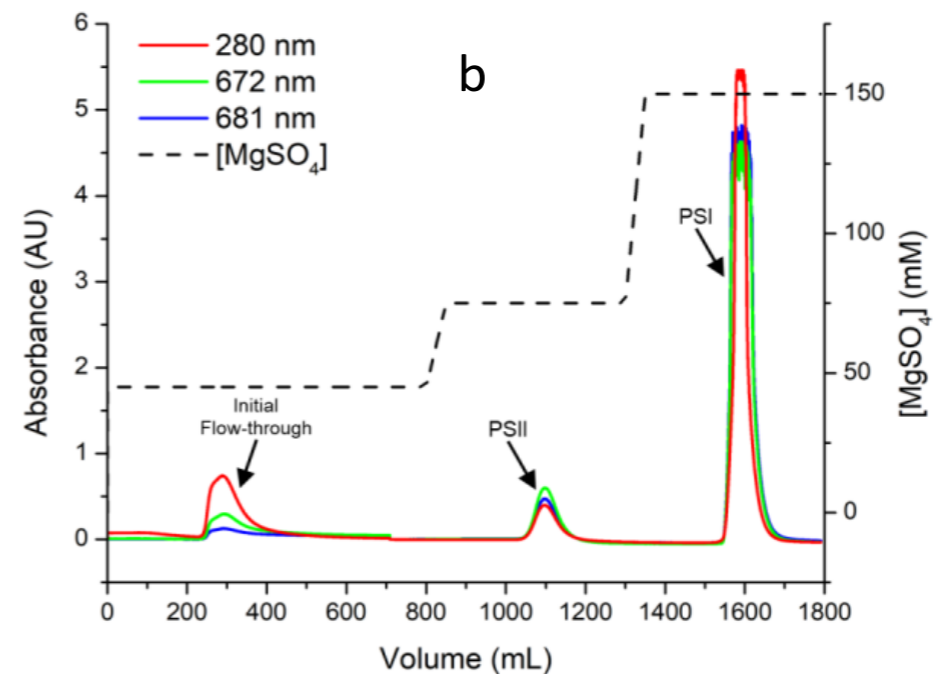
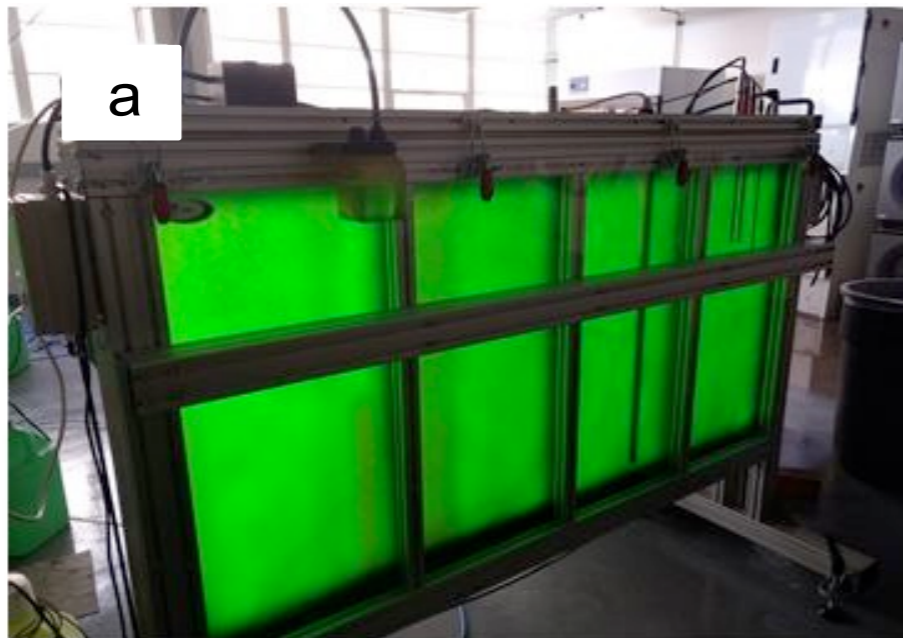
Figure from Wiedorn, M. O. et al. Megahertz serial crystallography. *Nat. Commun.* 9, 4025 (2018)

Henrich, B. et al. The adaptive gain integrating pixel detector **AGIPD** a detector for the European XFEL. *Nucl. Instrum. Methods Phys. Res. Sect. A Accel. Spectrometers, Detect. Assoc. Equip.* 633, S11–S14 (2011).

Allahgholi, A. et al. Megapixels @ Megahertz – the AGIPD high-speed cameras for the European XFEL. *Nucl. Instrum. Methods Phys. Res. Sect. A Accel. Spectrometers, Detect. Assoc. Equip.* 942, 162324 (2019)

PSI crystallization for SFX at EuXFEL

- over 1,000 mg of PSI were purified
- grew millions of uniformly sized ($5 \times 5 \times 15 \mu\text{m}^3$) microcrystals
- buffer: low ionic strength, i.e. low viscosity --> can jet well,
- less chance of clogging



Figures from Gisriel et al. Nat Comm. 10, 5021 (2019).

PSI crystallization for SFX at EuXFEL

Fromme lab, ASU

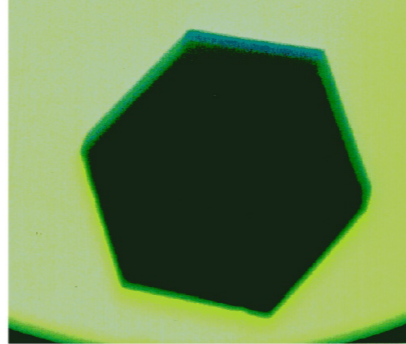
0.1 mm



1mm

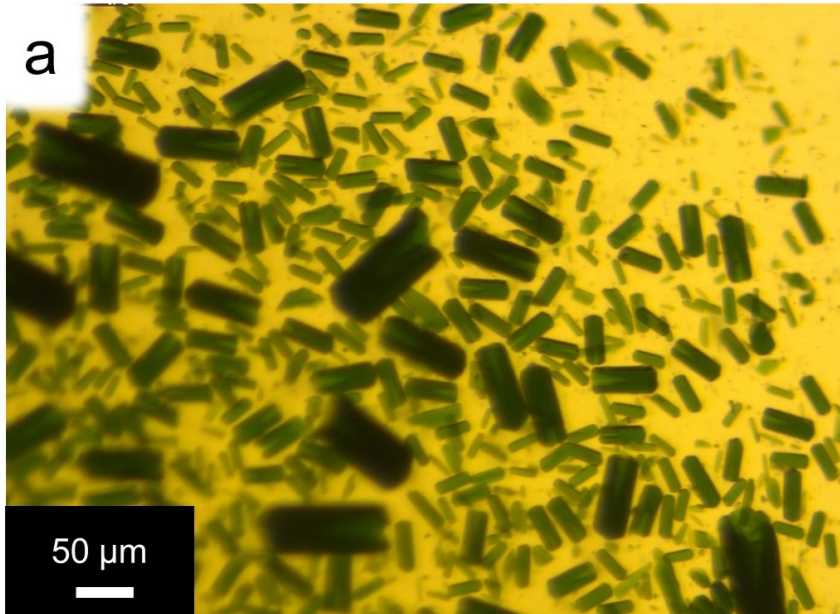


diameter: 1.5 mm

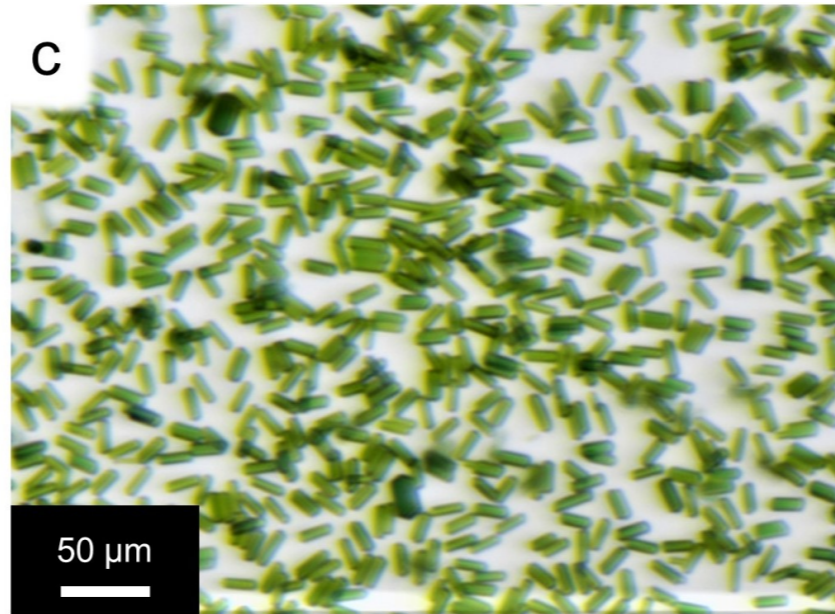


Microcrystal seeding can help grow large, high-quality PSI crystals, or large volumes of tiny, homogeneous crystals

a



c



GOAL: Homogeneous microcrystal solution

Fig. 3 PSI microcrystals. **a** Large size crystal distribution, grown by ultrafiltration. **b** uniform **5 x 5 x 15 μm PSI crystals** grown at the XBI user consortium laboratory by the **rotational agitation mixing with seeding** (RAMS) method.

Figures from:

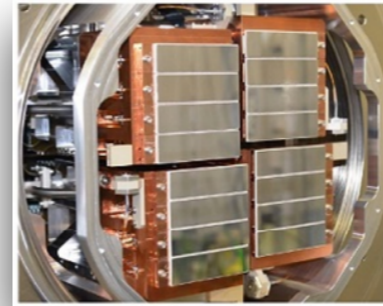
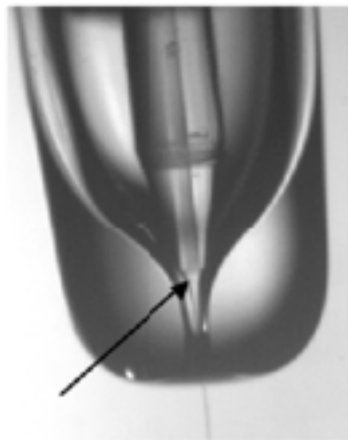
[top row] Roy Chowdhury from Fromme lab.

[bottom row] Gisriel et al. Nat Comm. 10, 5021 (2019)

Membrane protein (Photosystem I) MHz serial crystallography at the European XFEL

Sample delivery

- Micro crystals delivered in hand-made GDVN (gas-dynamic virtual nozzle) with 50 μm inner diameter,
 - made by Stella Lisova, ASU
- Flow rate: 20 $\mu\text{L}/\text{min}$
- Jet speed 50 m/s



Data collection

- 2nd experiment ever at EuXFEL: Sept 2017
- SPB/SFX beamline
- 9.3 keV X-rays
- 0.7 - 1.0 mJ average pulse energy
- $4.7 - 6.7 \times 10^{11}$ photons/pulse upstream
- 50% flux loss at sample position, estimated
- Beam focus: $16 \pm 4 \mu\text{m}$ (FWHM)
- 30-pulse trains at 10 Hz
- 50 fs pulse duration
- 886 ns pulse separation (1.13 MHz)

Indexing depends on detector distance

- Limited detector size and large pixels --> compromise between resolution limit and angular separation of Bragg reflections
- 1 MP detector with $200 \times 200 \mu\text{m}^2$ pixels
- This affects indexability and accuracy of local background calculations.

Table 1 Data collection statistics for PSI MHz SFX at the EuXFEL

Detector distance (cm)	32.7	23.3	Combined	Dark-state data (pulses 1-10 only)
Hit rate (%)	1.0	1.0	-1	-1
Hits	7900	51,112	59,012	19,023
Indexed patterns (30 pulses/train)	7403	47,377	54,780	18,176
Indexing rate	94%	93%	93%	96%
Resolution at the edge of the detector (Å), horizontal, vertical	4.1, 3.5	3, 2.6	Various	Various
Minimum peak separation (pixels)	7.6	5.4	Various	5-7

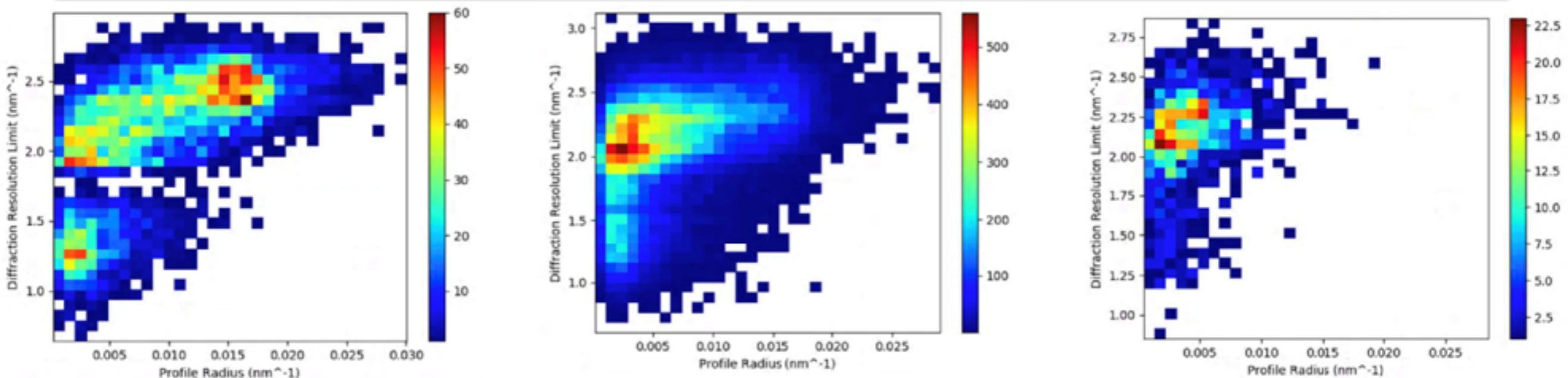
The data were used from two different detector positions. Only the first ten pulses of a given train contributed to the dark PSI structure determined here

Diffraction resolution limits of SFX PSI data collected at 3 sample-to-detector distances

0.327 m

0.233 m

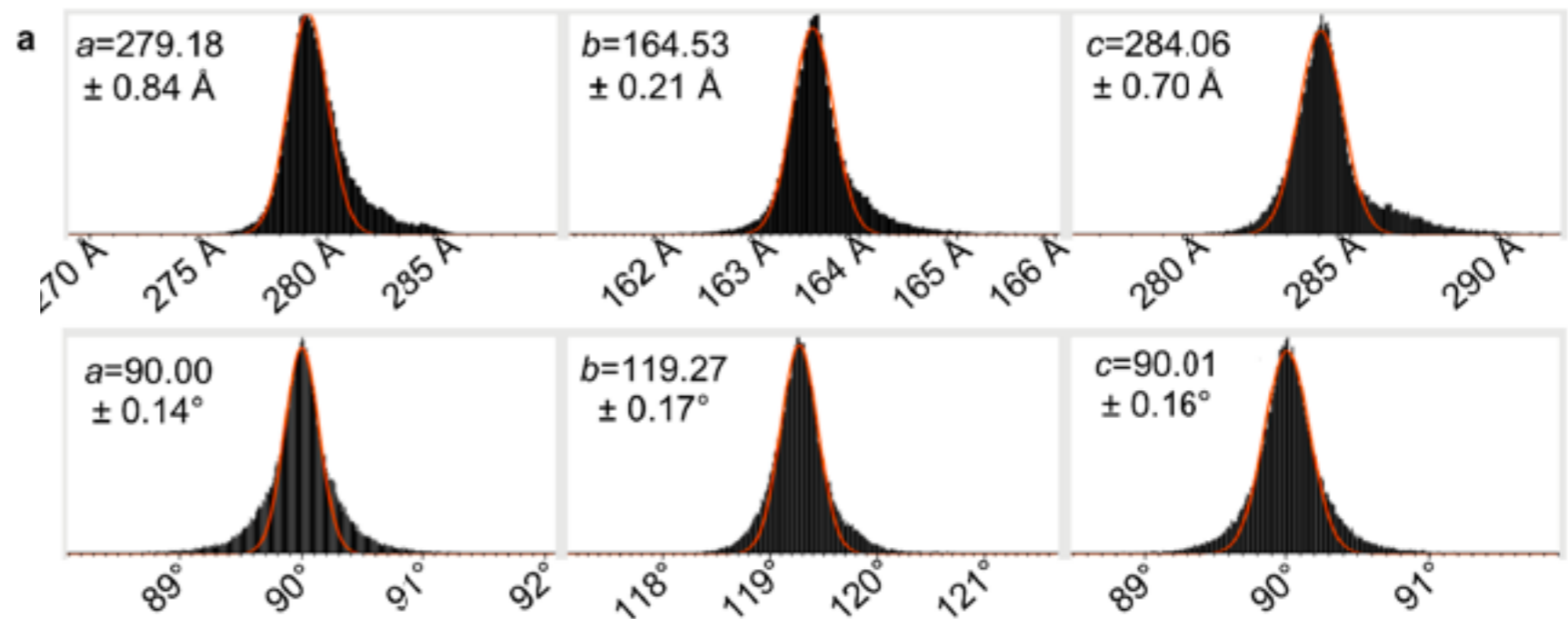
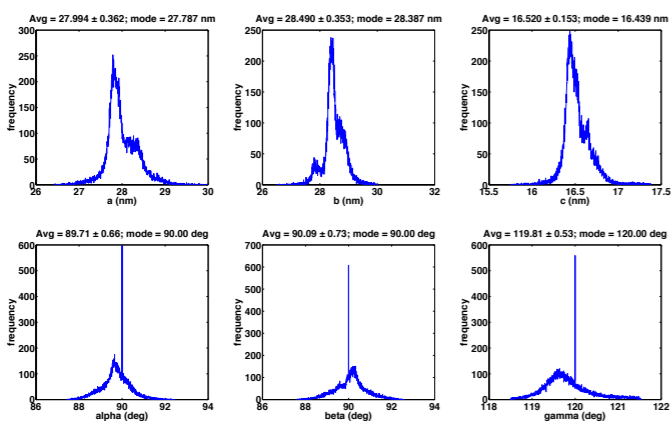
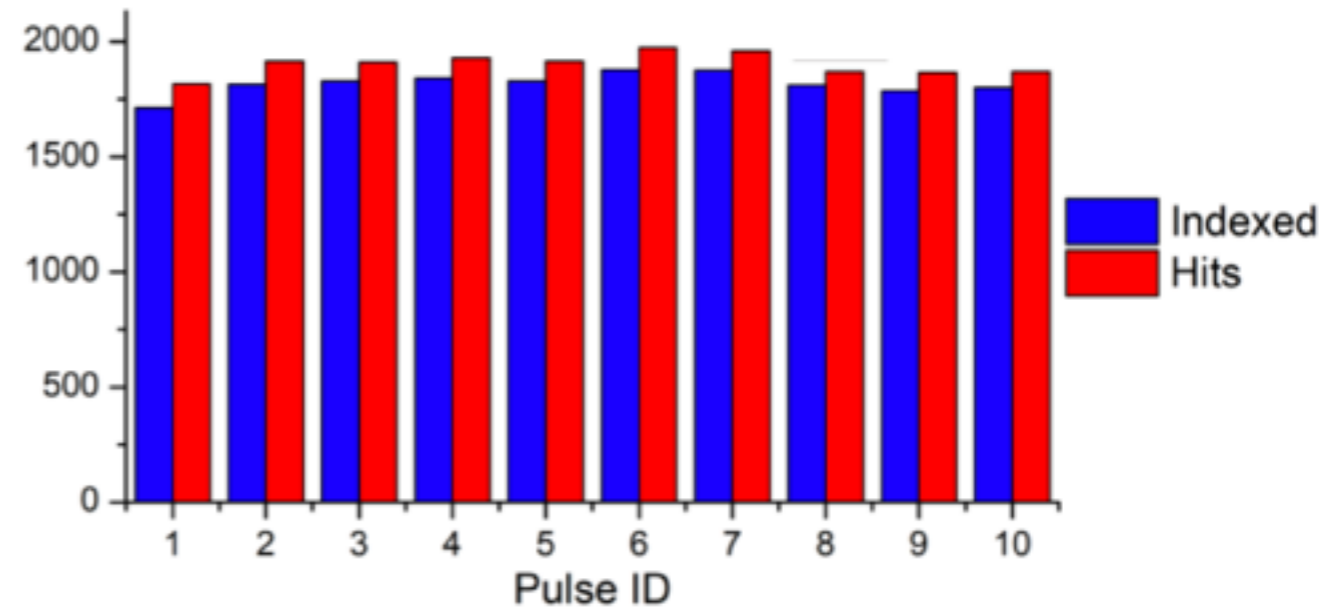
0.168 m



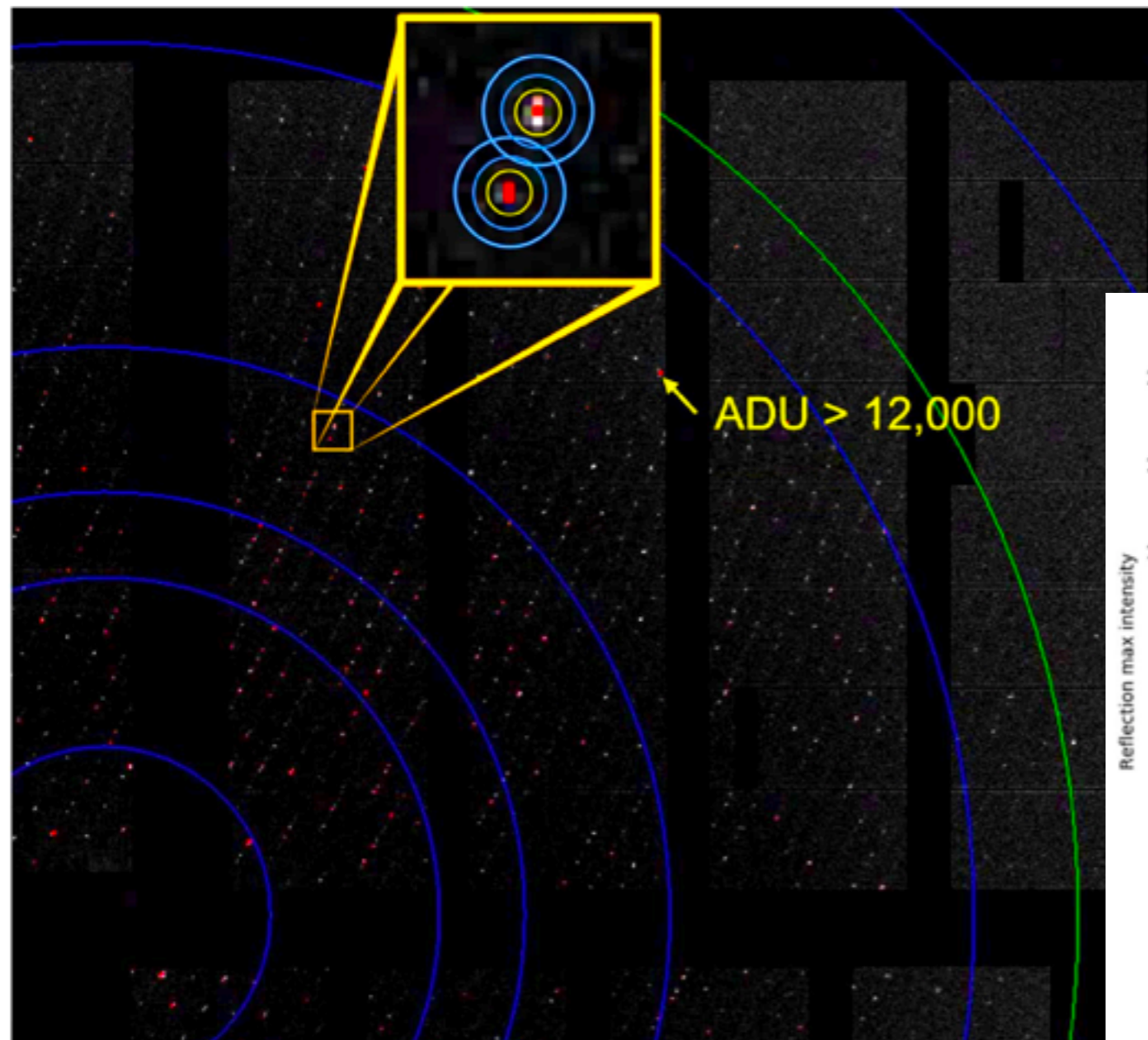
Membrane protein (Photosystem I) MHz serial crystallography at the European XFEL

Data analysis

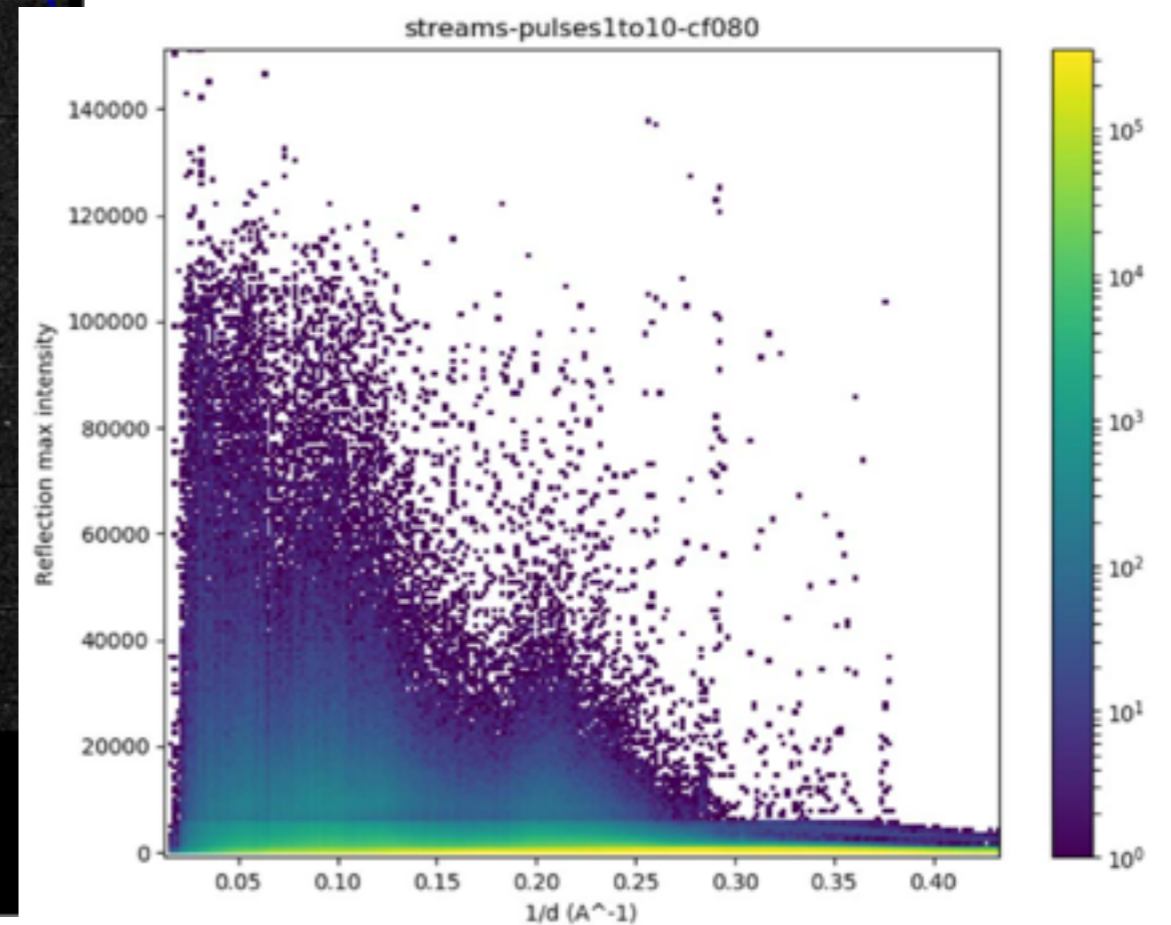
- Online monitoring: OnDA
- Hit finding and AGIPD calibration: Cheetah + Manuela Kuhn's code (DESY)
- Indexing: CrystFEL, Xgandalf
- Optimising: DatView
- Phasing & refinement: Phenix



AGIPD's high dynamic range allowed accurate measurements of Bragg reflection snapshots over the full resolution range



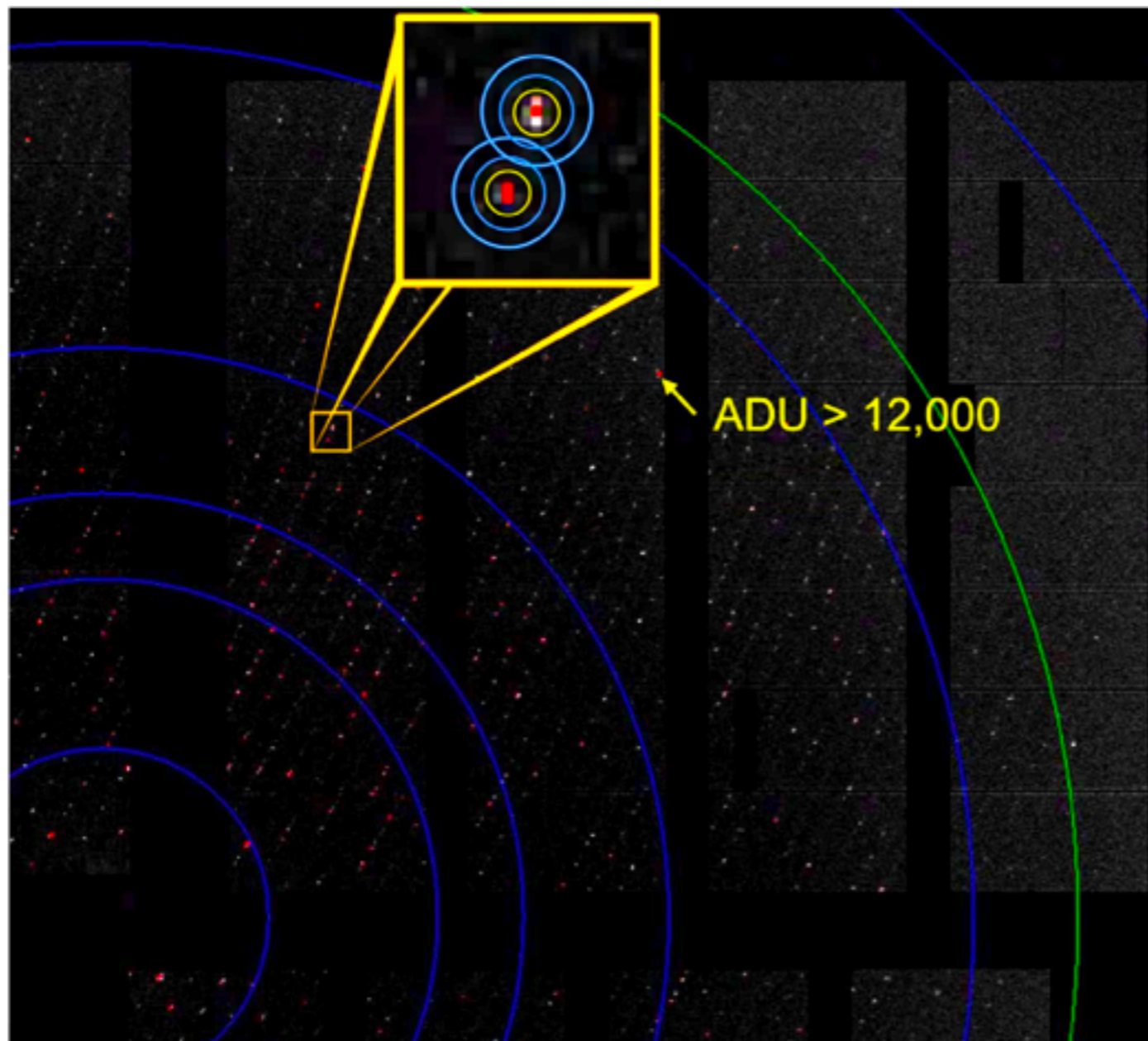
White pixels - high gain mode
Red pixels - medium or low gain



Henrich, B. et al. The adaptive gain integrating pixel detector AGIPD a detector for the European XFEL. Nucl. Instrum. Methods Phys. Res. Sect. A 633, S11–S14 (2011).

Figures from Gisriel et al. Nat Comm. 10, 5021 (2019).

AGIPD's high dynamic range allowed accurate measurements of Bragg reflection snapshots over the full resolution range



White pixels - high gain mode
Red pixels - medium or low gain

3-ring integration in CrystFEL

Local background estimate is less accurate due to closely spaced Bragg reflections (large unit cell)

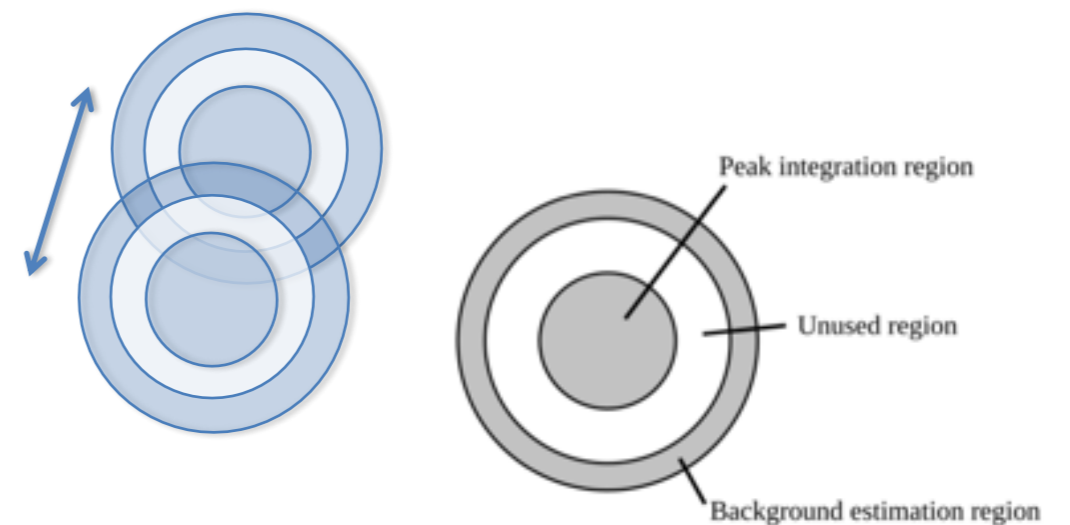
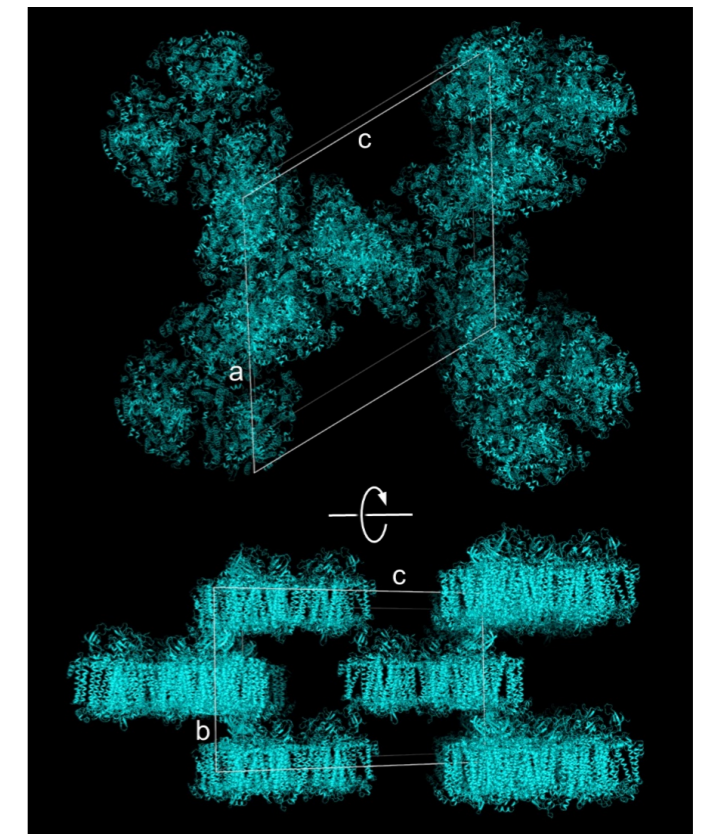
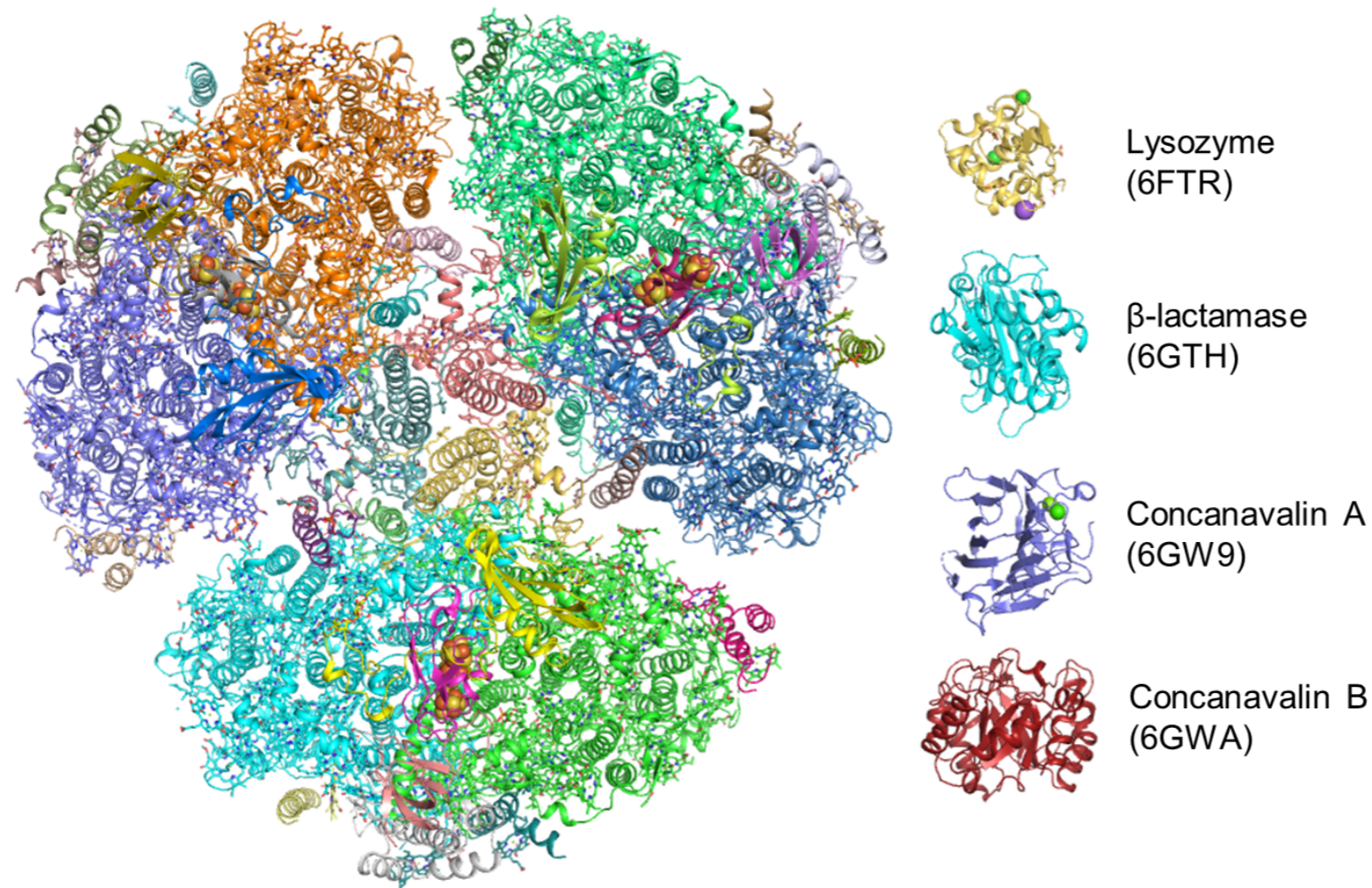


Figure from Gisriel et al. Nat Comm. 10, 5021 (2019).

White, T.A., et al. (2013). Crystallographic data processing for free-electron laser sources. Acta Cryst. D 69, 1231–1240.

Finally we confirmed cyanobacterial PSI is trimeric with a high-resolution SFX structure



PSI trimers in the crystal, showing the high (~78%) solvent content.

Fig. 4 (a) Trimeric PSI, a >1 MDa complex containing 36 protein subunits and 381 cofactors, with protein subunits colored individually, and 4 other structures determined using MHz SFX at the EuXFEL so far. (b) Views from the membrane plane (top) and membrane normal (bottom).

Figures from Gisriel et al. Nat Comm. 10, 5021 (2019).

Pseudo-hexagonal Photosystem I

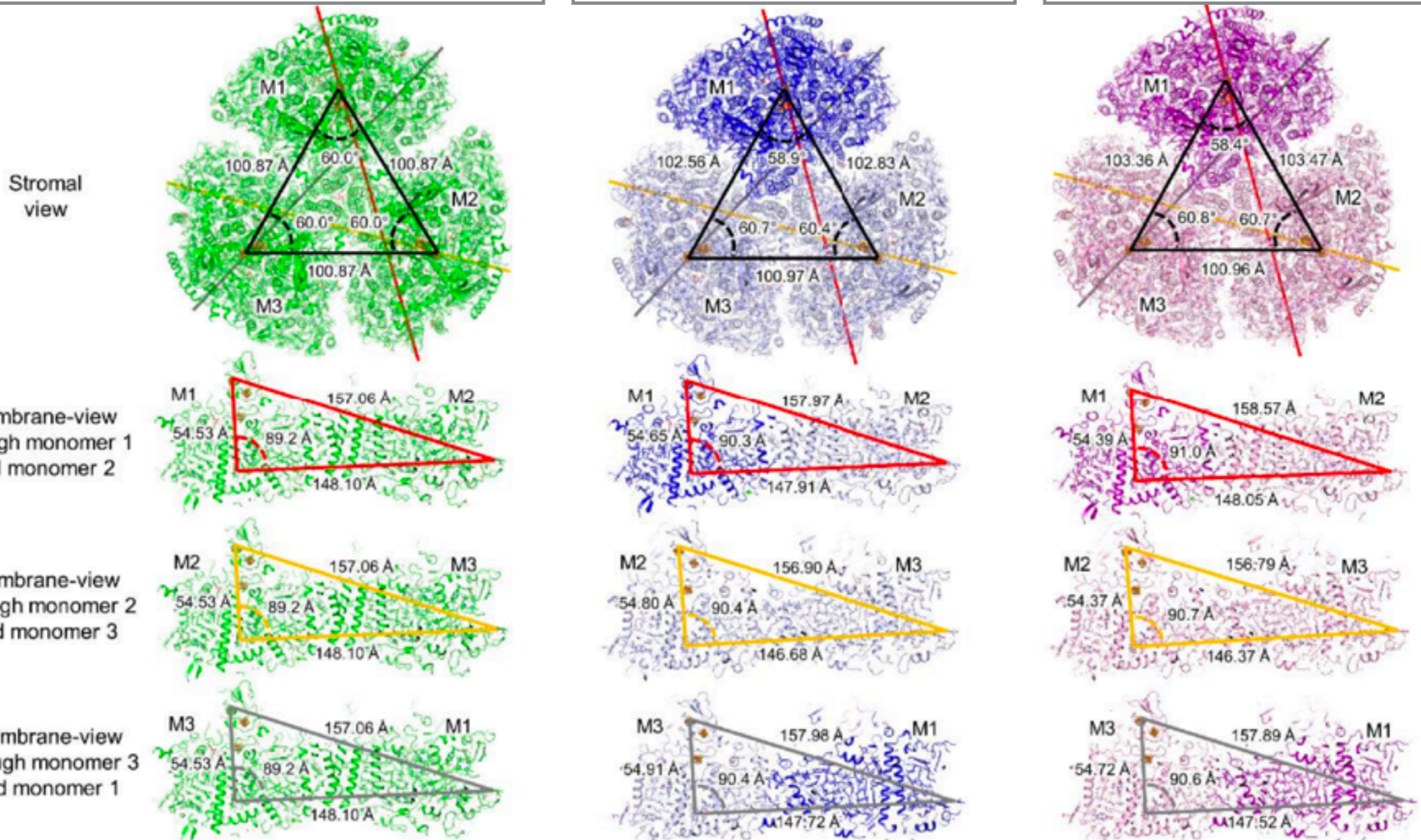
Trimer in P21 needs at least 3x more data than monomer in P63

Figures from Gisriel et al. Nat Comm. 10, 5021 (2019).

Published Cyanobacterial
cryo, synchrotron
PSI (1JB0) in P63

New cryo. PSI trimeric
structure from
synchrotron, in P21

Room temp.
EuXFEL structure
P21



Pseudo-hexagonal Photosystem I

Trimer in P21 needs at least 3x more data than monomer in P63

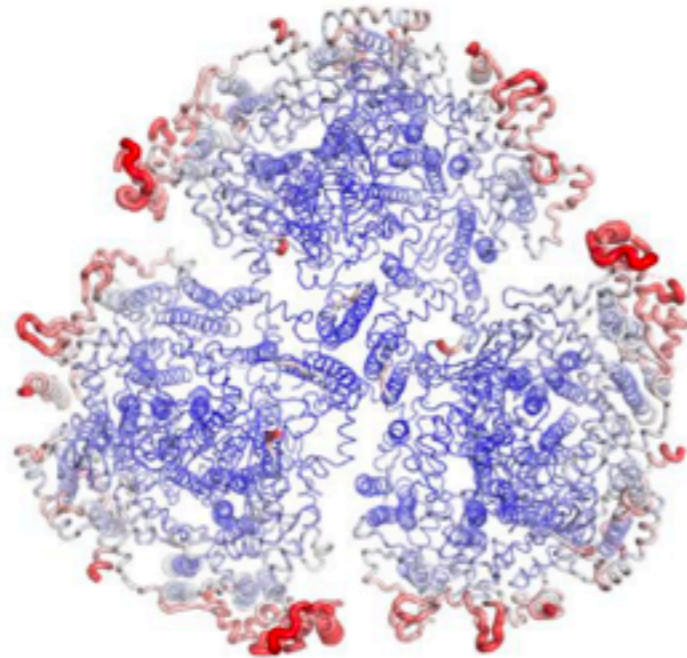
Figures from Gisriel et al. Nat Comm. 10, 5021 (2019).

Published Cyanobacterial
cryo, synchrotron
PSI (1JB0) in P63

New cryo. PSI trimeric
structure from
synchrotron, in P21

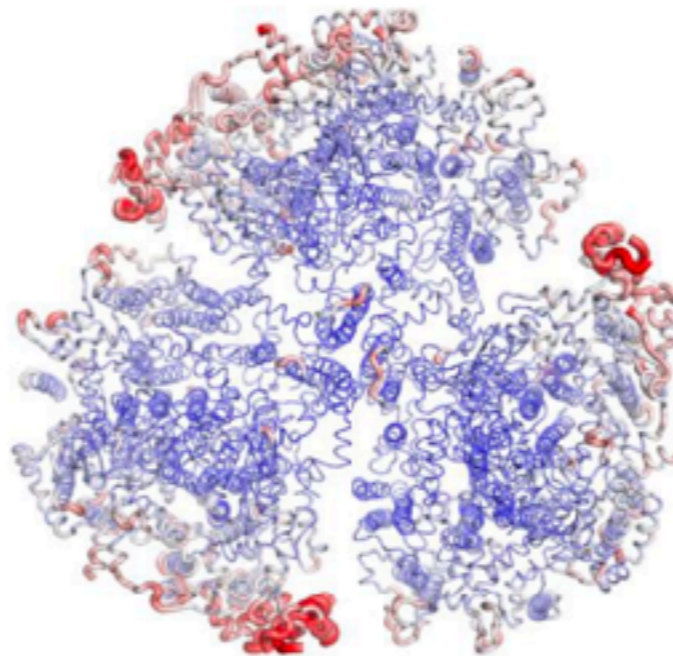
Room temp.
EuXFEL structure
P21

Cryogenic synchrotron
structure solved in P6₃



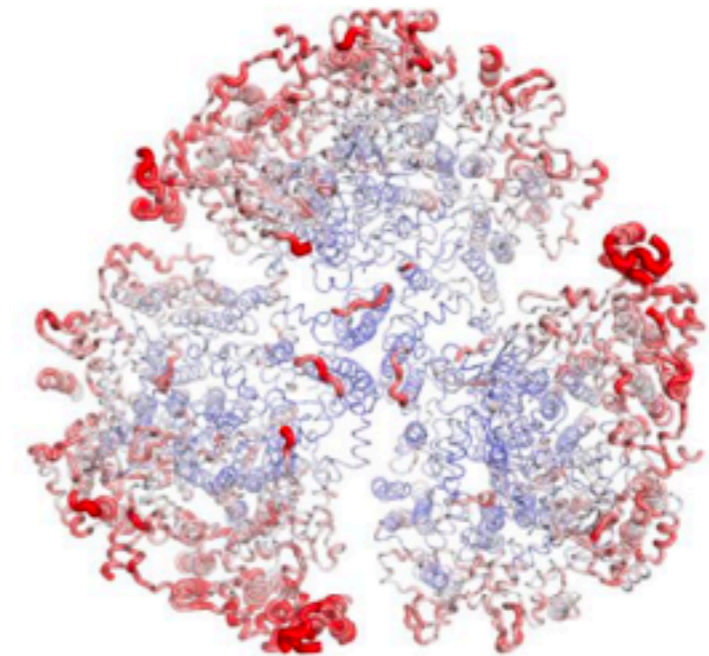
a = 286 Å
b = 286 Å,
c = 167 Å,
α = 90°
β = 90°,
γ = 120°

Cryogenic synchrotron
structure solved in P2₁



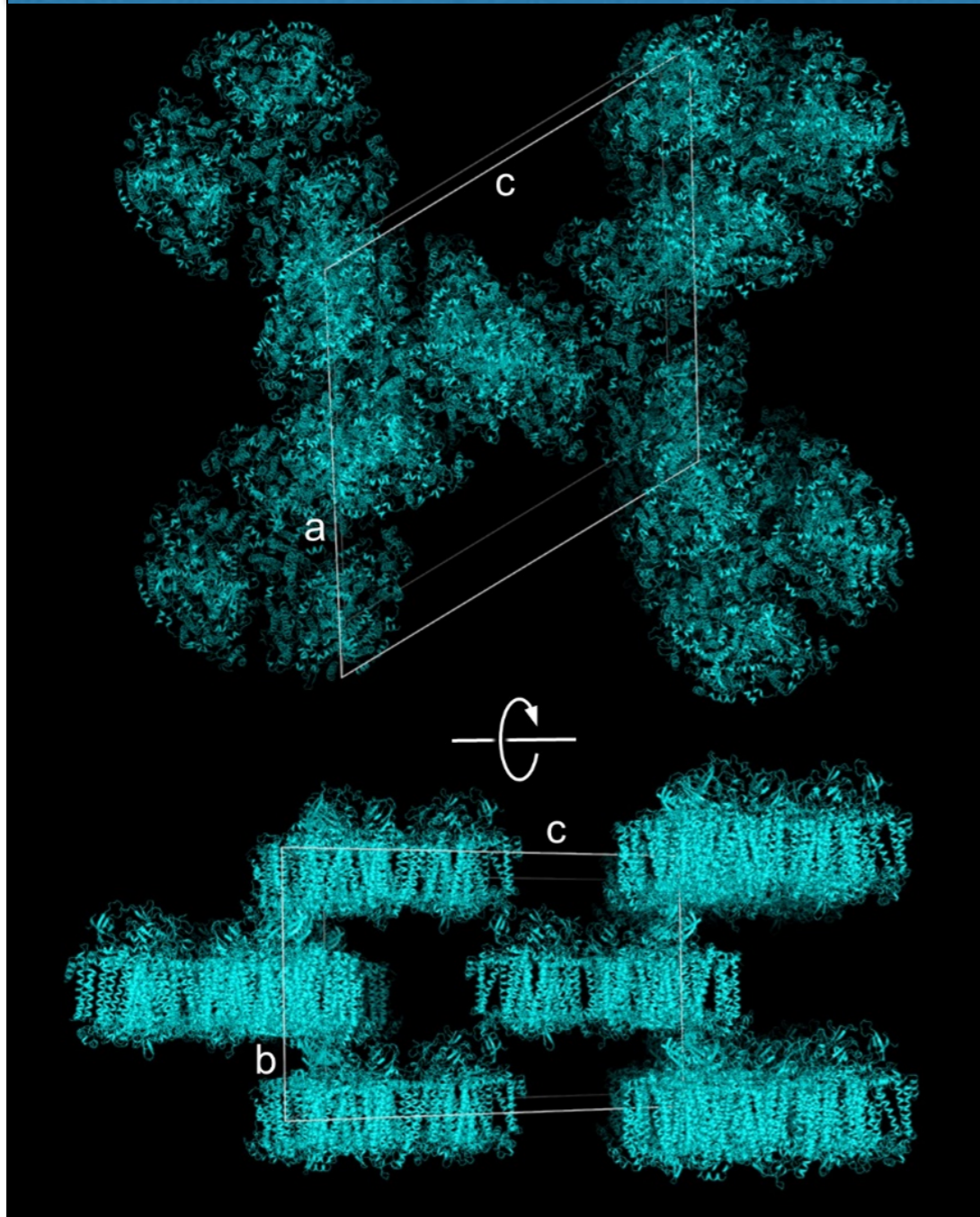
a = 278.5 Å
b = 165.1 Å,
c = 283.4 Å,
α = 90°,
β = 119.4°,
γ = 90°

RT XFEL
structure solved in P2₁



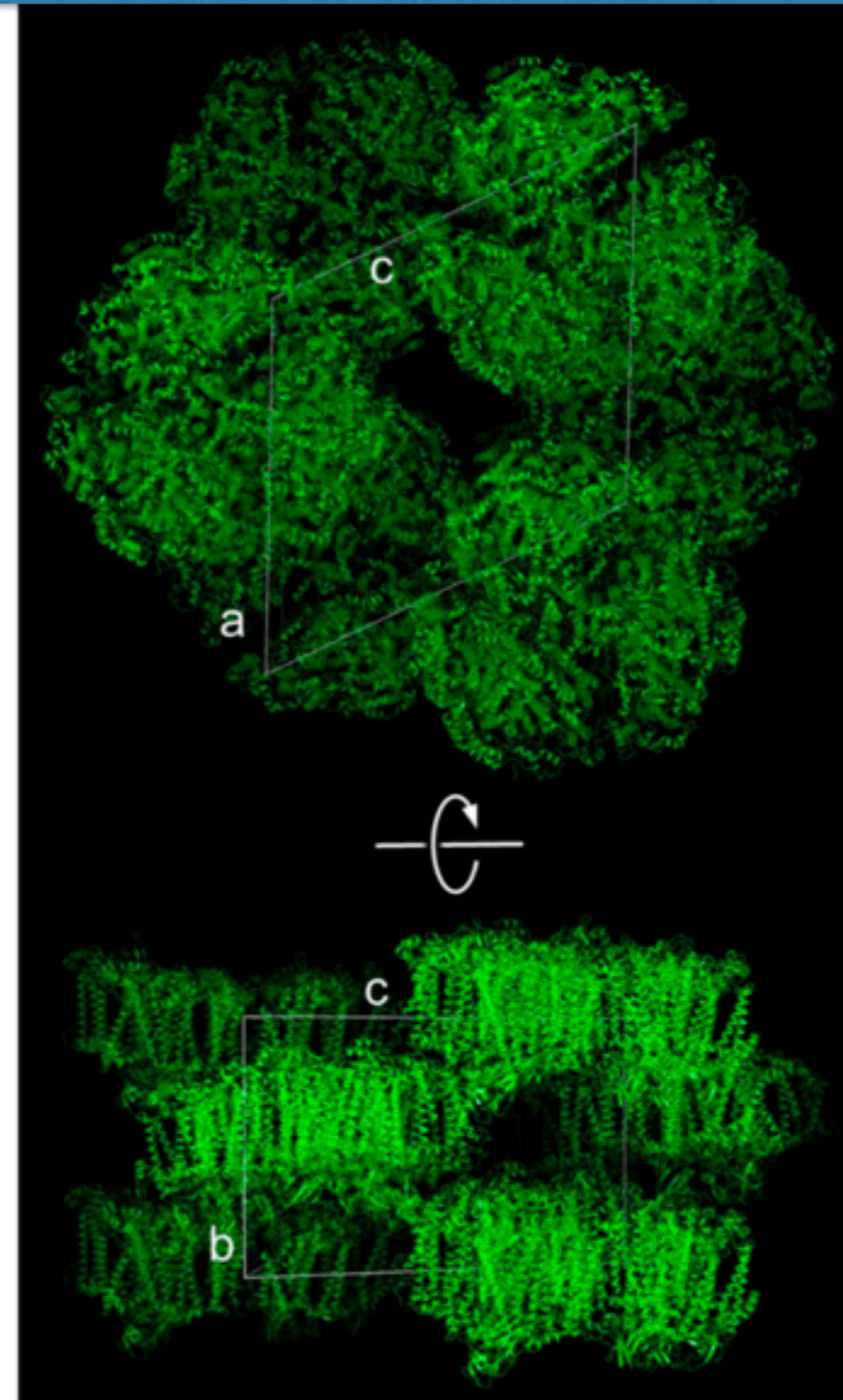
a = 279.2 Å
b = 164.5 Å
c = 284.1 Å,
α = 90°
β = 119.3 °
γ = 90°

Cyanobacterial PSI - comparing two different cyanobacterial PSI structures, in P2₁, with different crystal packing



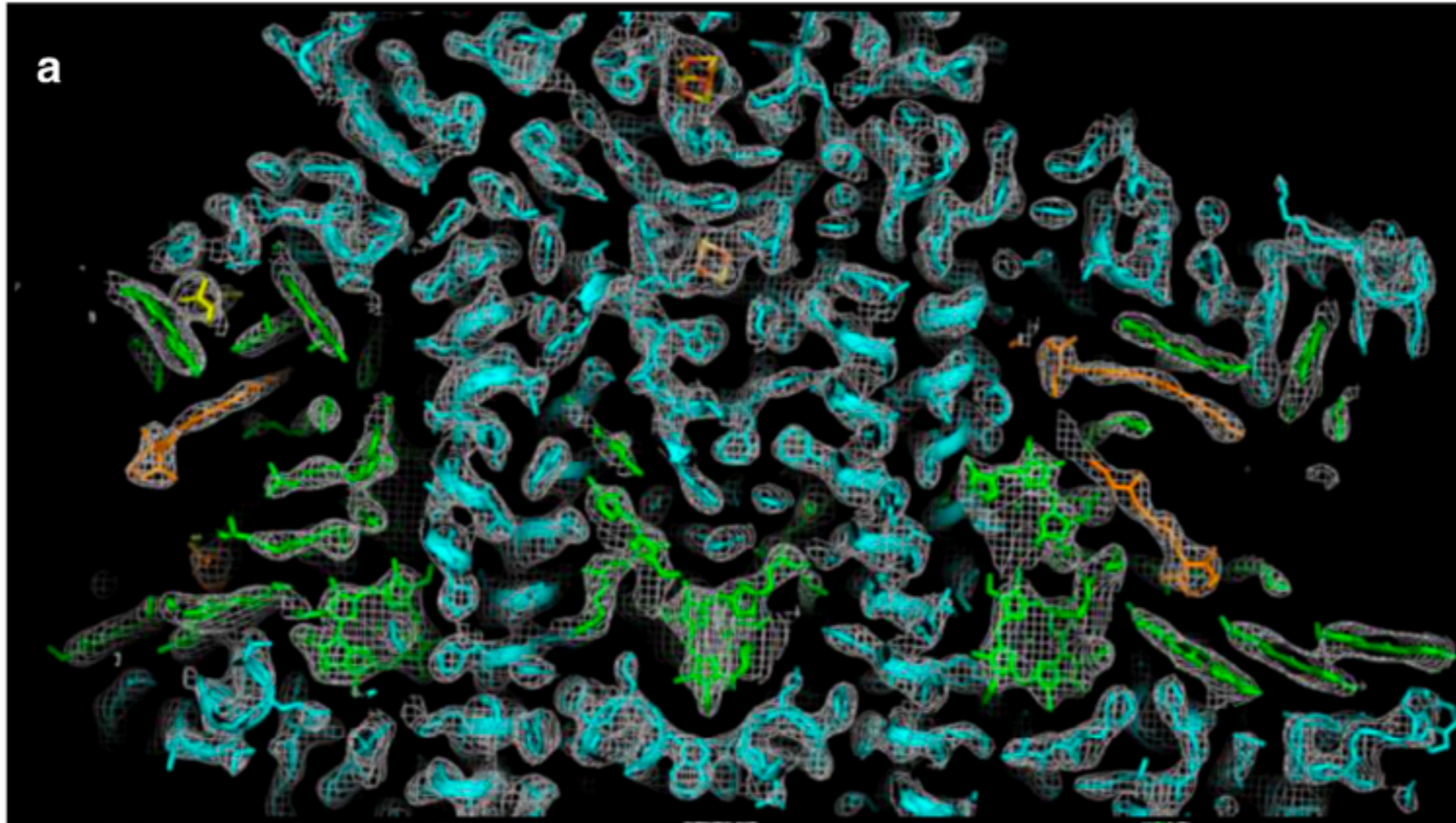
Packing of PSI in space group P2₁ from the structure of PSI from *T. elongatus*

Figures from Gisriel et al. Nat Comm. 10, 5021 (2019).



Packing of PSI in space group P2₁ from the structure of PSI from *S. sp.* PCC 6803 reported previously (PDB ID=5OY0)¹¹

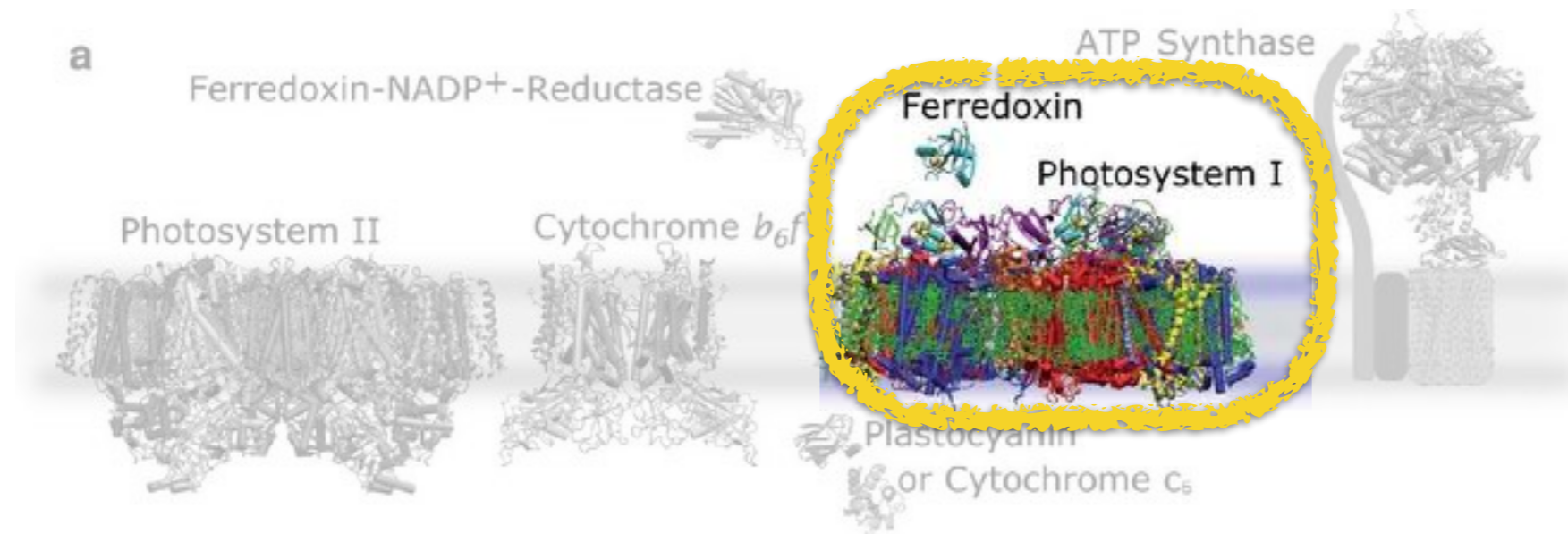
Photosystem I trimer structure



Electron density map ($2F_o - F_c$ at 1.5σ) and model of various PSI structural elements of the XFEL structure of PSI. In all images, protein is colored cyan, chlorophyll (Chl) molecules are colored green, β -carotenes are colored orange, and lipids are colored yellow.
(a) A slice through the center of electron density of a monomer of PSI.

Figure from Gisriel et al. Nat Comm. 10, 5021 (2019).

Coming soon: pump-probe MHz SFX from Photosystem I-Ferredoxin



- **Next challenge - time-resolved structures from electrons transfer from PSI to Ferredoxin**
- **We will need much more data!**
- **MHz rates at EuXFEL will really be crucial.**

Fromme lab

Figure from Ch. 1 Fromme & Grotjohann in Fromme P (ed.) Photosynthetic Protein Complexes: A Structural Approach. Wiley-Blackwell; 2008

Thank you!

Chris Gisriel^{1,2,23,26}, Jesse Coe^{1,2,26}, Romain Letrun³, Oleksandr M. Yefanov⁴, Cesar Lunda-Chavez^{1,2}, Natasha E. Stander^{1,2}, Stella Lisova^{1,5}, Valerio Mariani⁴, Manuela Kuhn⁴, Steve Aplin⁴, Thomas D. Grant^{6,7}, Katerina Dörner³, Tokushi Sato^{3,4}, Austin Echelmeier^{1,2}, Jorvani Cruz Villarreal^{1,2}, Mark S. Hunter⁸, Max O. Wiedorn^{4,9,10}, Juraj Knoska⁴, Victoria Mazalova⁴, Shatabdi Roy-Chowdhury^{1,2}, Jay-How Yang^{1,2}, Alex Jones^{1,2}, Richard Bean³, Johan Bielecki³, Yoonhee Kim³, Grant Mills³, Britta Weinhausen³, Jose D. Meza³, Nasser Al-Qudami³, Saša Bajt¹¹, Gerrit Brehm^{1,2,12,13}, Sabine Botha⁵, Djelloul Boukhelef³, Sandor Brockhauser^{3,14}, Barry D. Bruce^{15,16,17}, Matthew A. Coleman¹⁸, Cyril Danilevski³, Erin Discianno¹, Zachary Dobson^{1,2}, Hans Fangohr^{3,19}, Jose M. Martin-Garcia¹, Yaroslav Gevorkov^{4,20}, Steffen Hauf³, Ahmad Hosseinizadeh²¹, Friederike Januschek^{3,24}, Gihan K. Ketawala^{1,2}, Christopher Kupitz^{8,21}, Luis Maia³, Maurizio Manetti³, Marc Messerschmidt^{1,2,3}, Thomas Michelat³, Jyotirmoy Mondal¹⁵, Abbas Ourmazd²¹, Gianpietro Previtali³, Iosifina Sarrou⁴, Silvan Schön⁴, Peter Schwander²¹, Megan L. Shelby¹⁸, Alessandro Silenzi³, Jolanta Sztuk-Dambietz³, Janusz Szuba³, Monica Turcato³, Thomas A. White⁴, Krzysztof Wrona³, Chen Xu³, Mohamed H. Abdellatif⁴, James D. Zook^{1,2}, John C.H. Spence^{1,5}, Henry N. Chapman^{4,9,10}, Anton Barty⁴, Richard A. Kirian^{1,5}, Matthias Frank¹⁸, Alexandra Ros^{1,2}, Marius Schmidt²¹, Raimund Fromme^{1,2}, Adrian P. Mancuso^{3,22}, Petra Fromme^{1,2*} & Nadia A. Zatsepin^{1,5,25*}

¹Biodesign Center for Applied Structural Discovery, Arizona State University, Tempe, AZ 85287-5001, USA. ²School of Molecular Sciences, Arizona State University, Tempe, AZ 85287-1604, USA. ³European XFEL GmbH, Holzkoppel 4, 22869 Schenefeld, Germany. ⁴Center for Free-Electron Laser Science, Deutsches Elektronen-Synchrotron, Notkestrasse 85, 22607 Hamburg, Germany. ⁵Department of Physics, Arizona State University, Tempe, AZ 85287-1504, USA. ⁶Hauptman-Woodward Institute, 700 Ellicott St, Buffalo, NY 14203-1102, USA. ⁷Department of Structural Biology, Jacobs School of Medicine and Biomedical Sciences, SUNY University at Buffalo, 700 Ellicott St, Buffalo, NY 14203-1102, USA. ⁸Linac Coherent Light Source, SLAC National Accelerator Laboratory, Menlo Park 94025 CA, USA. ⁹Department of Physics, Universität Hamburg, Luruper Chaussee 149, 22761 Hamburg, Germany. ¹⁰The Hamburg Centre for Ultrafast Imaging, Universität Hamburg, Luruper Chaussee 149, 22761 Hamburg, Germany. ¹¹Deutsches Elektronen-Synchrotron, Notkestrasse 85, 22607 Hamburg, Germany. ¹²Institute for X-Ray Physics, University of Göttingen, 37077 Göttingen, Germany. ¹³Center Nanoscale Microscopy and Molecular Physiology of the Brain, Göttingen, Germany. ¹⁴Biological Research Centre, Hungarian Academy of Sciences, Temesvári krt. 62, Szeged 6726, Hungary. ¹⁵Department of Biochemistry & Cellular and Molecular Biology, University of Tennessee at Knoxville, Knoxville, TN, USA 37996. ¹⁶Program in Energy Science and Engineering, University of Tennessee at Knoxville, Knoxville, TN, USA 37996. ¹⁷Department of Microbiology, University of Tennessee at Knoxville, Knoxville, TN, USA 37996. ¹⁸Lawrence Livermore National Laboratory, 7000 East Avenue, Livermore, CA 94550, USA. ¹⁹University of Southampton, University Rd, Southampton SO17 1BJ, UK. ²⁰Hamburg University of Technology, Vision Systems E-2, Harburger Schloßstraße 20, 21079 Hamburg, Germany. ²¹Department of Physics, University of Wisconsin-Milwaukee, 3135 N. Maryland Ave, Milwaukee, WI 53211, USA. ²²Department of Chemistry and Physics, La Trobe Institute for Molecular Science, La Trobe University, Melbourne 3086 Victoria, Australia. ²³Present address: Department of Chemistry, Yale University, New Haven, CT 06520, USA. ²⁴Present address: Deutsches Elektronen-Synchrotron, Notkestrasse 85, 22607 Hamburg, Germany. ²⁵Present address: Department of Chemistry and Physics, La Trobe Institute for Molecular Science, La Trobe University, Melbourne 3086 Victoria, Australia. ²⁶These authors contributed equally: Chris Gisriel, Jesse Coe.

